SAN FRANCISCO ESTUARY & WATERSHED SCIENCE
Sponsored by the Delta Science Program and the UC Davis Muir Institute

RESEARCH

Statistical Evaluation of Behavior and Population Dynamics Models that Predict Movement and Proportional Entrainment Loss of Adult Delta Smelt in the Sacramento–San Joaquin River Delta

Josh Korman*[1], Edward S. Gross[2], Lenny F. Grimaldo[3]

ABSTRACT

There has been considerable debate about effects of entrainment of endangered Delta Smelt (*Hypomesus transpacificus*) at water export facilities located in the Sacramento–San Joaquin River Delta. In this paper we use a behavior-driven movement model (BMM) to simulate the movement of adult Delta Smelt, which, in conjunction with a population dynamics model, estimates the proportion of the population that is lost to entrainment, i.e., proportional entrainment loss (PEL). Parameters of the population model are estimated by maximum likelihood by comparing predictions to data from Fall Midwater Trawl (FMWT) and Spring Kodiak Trawl (SKT) surveys, as well as to daily salvage estimates. Our objectives are to evaluate different movement behavior hypotheses, to rank estimates of PEL based on how well predictions fit the data, and to sharpen our understanding of the data to inform future research and monitoring decisions.

We applied the modeling framework to data from water year 2002—a year when salvage was high—and tested 30 combinations of six behavior and five population dynamics models. More complex process and observation assumptions in the population model led to much improved fits in most cases, but did not appreciably influence PEL predictions, which were largely determined by movement predictions from the BMMs. Estimates of PEL varied considerably among behaviors (2% to 40%). The model with the highest predictive capability explained 98% of the variation in FMWT data across regions, 70% of the variation in SKT data across regions and surveys, and 28% and 43% of the daily variation in salvage at federal and state fish screening facilities, respectively. The PEL estimate from this model was 35%, more than double the original estimate from Kimmerer (2008) of 15%. While PEL estimates provided in this study should be considered preliminary, our framework for testing combined behavior-driven movement models and population dynamics models is an improvement compared to earlier efforts.

SFEWS Volume 19 | Issue 1 | Article 1

https://doi.org/10.15447/sfews.2021v19iss1art1

* Corresponding author: *jkorman@ecometric.com*

1 Ecometric Research
Vancouver, BC, V6S 1J3

2 Resource Management Associates
Walnut Creek, CA 94596, and
Center for Watershed Sciences
University of California Davis
Davis, CA, 95616 USA

3 ICF, San Francisco, CA 94107 USA
Current address:
California Department of Water Resources
Sacramento, CA 95814 USA

KEY WORDS

entrainment, Delta Smelt, fish movement, particle-tracking models, population models

INTRODUCTION

Worldwide, over 58,000 dams and diversion structures (>15 m height) have been constructed to provide water supply, flood control, and hydroelectric power generation (ICOLD 2015). The presence and operations of these facilities can adversely affect native fish populations through habitat fragmentation, reductions in habitat quantity and quality, enhancement of non-native species, and direct losses from entrainment mortality (Rytwinski et al. 2017). Entrainment loss is one of the most obvious effects because it is often easily observed through tagging, fish sampling in diverted water, or collection of dead fish on screens and louvers. Entrainment loss can trigger protective management actions intended to eliminate or minimize destruction of fish or "take," as specified in the US Endangered Species Act (ESA). Significant efforts to quantify and reduce mortality associated with entrainment have been undertaken in a number of large river systems including the Hudson River (Barnthouse et al. 1988), the Columbia River (Simpson 2018), and the Sacramento-San Joaquin River Delta (Kimmerer 2008). The net effect of entrainment on the viability of fish populations has been challenging to determine, in part because the proportion of the population that is lost to entrainment is often not known. This uncertainty hampers evaluation of entrainment reduction measures.

Entrainment of Delta Smelt (*Hypomesus transpacificus*) and other fish at water export facilities located in the Sacramento-San Joaquin River Delta, and associated export constraining regulatory measures, have led to intensive study and debate about the effects of entrainment on the viability of the population (Kimmerer 2008, 2011; Brown et al. 2009; Miller 2011). Delta Smelt is a small pelagic fish endemic to the San Francisco Estuary (Bennett 2005). Abundance of this species declined in the 1980s, and it was listed as threatened under both California and federal Endangered Species Acts in 1993. A rapid and sustained drop in Delta Smelt abundance beginning in ca. 2002—coincident with the decline of other pelagic species (the Pelagic Organism Decline; Sommer et al. 2007; Mac Nally et al. 2010)—resulted in the listing being revised to endangered under the California ESA in 2009. Over their annual life cycle, Delta Smelt typically spend the summer and fall in tidally-fresh to low-salinity waters (0 to 6 practical salinity units) of Suisun Bay and the western and northern portions of the Sacramento-San Joaquin Delta (hereafter referred to as the "Delta," Figure 1). In anticipation of spring spawning, a landward migration into less saline water is believed to occur for a component of the population (Grimaldo et al. 2009; Sommer et al. 2011). This movement is thought to be triggered by higher inflows and turbidity caused by the first large precipitation event in winter, referred to as the "first flush" (Grimaldo et al. 2009).

The Delta is a key part of the water supply for California. Water from the Sacramento and San Joaquin river drainages flows into the Delta, and, on average, approximately 30% of this inflow is diverted through massive state (State Water Project; SWP) and federal (Central Valley Project; CVP) export pumping facilities (Kimmerer 2004; Thomson et al. 2010) to supply water for about 25 million Californians and a multi-billion-dollar agricultural industry (Thomson et al. 2010). These pumping facilities, located at the southwestern edge of the Delta (Figure 1), alter seasonal patterns in the net direction of freshwater flow, and have entrained large numbers of Delta Smelt and other fish species under certain hydrodynamic, physical, and biological conditions (Kimmerer 2008; Grimaldo et al. 2009). The diversion often causes water in the lower San Joaquin River and Old and Middle rivers (OMR) to move toward the pumps instead of the ocean (often termed "reverse flows"), and draws water from the Sacramento River across the Delta, rather than follow its more norther natural route to the ocean (Figure 1). The landward migration of Delta Smelt results in some of the population moving closer to areas of altered flows and the pumping facilities, which makes them more

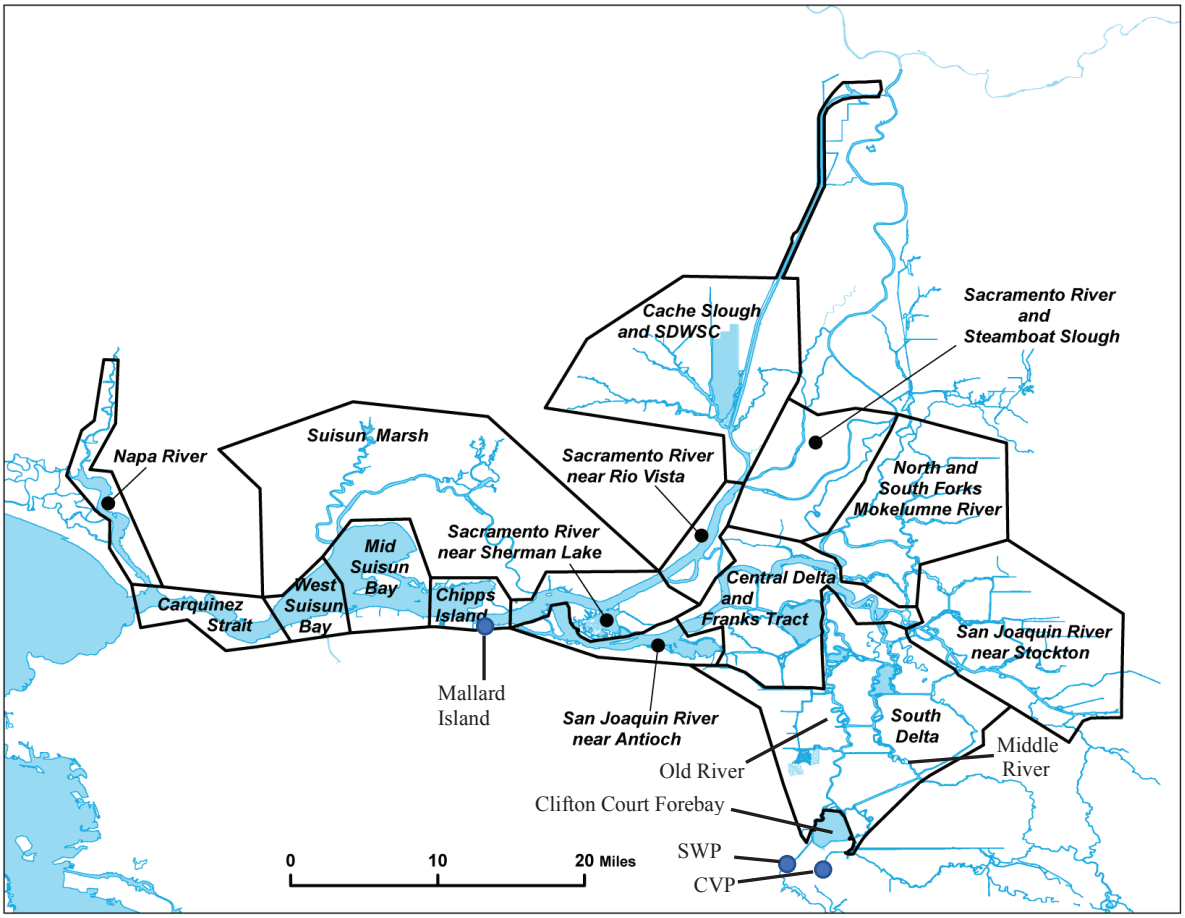

Figure 1 The San Francisco Bay-Delta, showing the boundaries of regions used in this study and the location of the State Water Project (SWP) and the federal Central Valley Project (CVP) fish-screen facilities and pumping plants.

vulnerable to entrainment, particularly when flow directions are reversed. Fish screening facilities located adjacent to the pumping plants collect some of the fish that would otherwise be entrained into the pumps. These collections, known as "salvage," provide a valuable but imperfect index of seasonal and annual variation in entrainment (Castillo et al. 2014). Salvage represents only a portion of total entrainment because some entrained fish reach the fish screening facilities but are not diverted by the screens (as determined by facility efficiency), while others die from predation before reaching the screens (pre-screen loss). Entrainment has been calculated by multiplying the observed salvage by an uncertain "salvage expansion factor," which is intended to account for the effects of both facility effeciency and pre-screen loss (Kimmerer 2008, 2011; Miller 2011).

Entrainment of Delta Smelt has been implicated as one of the potential causes for its decline (Sommer et al. 2007; Brown et al. 2009; MacNally et al. 2010). Concern over the effects of entrainment losses prompted the US Fish and Wildlife Service (USFWS) to issue a Biological Opinion on the SWP and CVP with targeted Reasonable and Prudent Alternative (RPA) actions designed to minimize Delta Smelt entrainment (USFWS 2008). Mandated pumping and flow prescriptions may result in substantial reductions in the SWP and CVP water diversions, and have been the subject of considerable litigation (Wanger 2007, 2010). A better understanding of the migratory dynamics of Delta Smelt and the effect of flows

https://doi.org/10.15447/sfews.2021v19iss1art1

on entrainment is warranted to evaluate the effectiveness of current and future flow and water export options (Sommer et al. 2011). Improved estimates of Delta Smelt entrainment losses are also needed to understand how water exports may affect population viability and recovery (e.g., Maunder and Deriso 2011; Rose et al. 2013). Kimmerer (2008) provided the first published estimates of the proportion of the population lost to entrainment, most commonly referred to as proportional entrainment loss (PEL). His estimates of the adult population of Delta Smelt was as high as 50% in 1 year, and indicated that entrainment could be having substantive population-level effects. These initial estimates have been the subject of debate (Miller 2011; Kimmerer 2011), and there is continued interest in reducing the uncertainty associated with Delta Smelt entrainment and estimates of PEL.

To date, proportional entrainment loss for adult Delta Smelt has been calculated based on the ratio of estimated entrainment to estimated population size (Kimmerer 2008, 2011; Miller 2011). Entrainment was calculated by inflating the estimated salvage using a salvage expansion factor. Population size was calculated by expanding catches from a Delta-wide scientific survey used to index abundance. There are two limitations to this approach for estimating PEL. First, it relies on uncertain expansion factors to calculate entrainment and population size. Second, historical estimates of PEL depend on the magnitude and timing of inflow, export rates, and other conditions in each year. Statistical separation of these factors can be difficult, leading to greater uncertainty in predictions of PEL under future operations and flow conditions.

Combined behavior and particle-tracking models provide a potentially more reliable way to predict the effects of alternative operations on entrainment losses. These models simulate movement of particles as determined by hydrodynamic predictions and other factors thought to cue fish movement and distribution such as salinity, water temperature, and turbidity. The majority of these models simulate the distribution of ichthyoplankton in coastal and estuarine areas to evaluate the effects of entrainment from power plants (Blumberg et al. 2004; Heimbuch et al. 2007; White et al. 2010), or the effects of dispersal to different coastal areas on the survival rate of early life stages and the resulting effect on recruitment (Hinrichsen et al. 2011). In most applications, the target organisms are assumed to behave as passively drifting particles or to exhibit very simple vertical swimming behaviors (e.g., North et al. 2008). Particle-tracking models have been used to predict entrainment in the Delta, especially for zooplankton and eggs and larval stages of Delta Smelt and other fishes that are assumed to behave as passively drifting particles (Culberson et al. 2004; Kimmerer and Nobriga 2008). It is unlikely that passive transport is an accurate way to model movement and entrainment vulnerability for older life stages of fish that exhibit a variety of complex behaviors. Our model is relatively unusual because it simulates a variety of movement behaviors driven by different abiotic drivers such as flow direction, and velocity and turbidity levels and gradients.

The central objective of the work presented here is to evaluate whether BMMs can predict abundance, distribution, and salvage observations, and in turn produce more reliable estimates of PEL for adult Delta Smelt. Our approach differs from past efforts (e.g., Rose et al. 2013) because we focus on testing predictions by comparing them directly to data. We use a two-stage modeling procedure. A computationally intensive behavior and particle-tracking model simulates a variety of potential behaviors of Delta Smelt to predict movement of particles among regions in the Delta as well as the proportion of particles from each region that are entrained. These predictions are based on behavioral rules that represent different hypotheses about how Delta Smelt respond to hydrodynamics (depth, velocity, and tidal flow direction), salinity, and turbidity. A key advantage of this approach is that it allows us to evaluate hypotheses about factors that affect Delta Smelt movement and distribution which are not well understood but represent a key management issue (Sommer et al. 2011; Bennett and Burau 2015). Proportional entrainment

predictions from the BMM are unscaled or naïve in the sense that they do not account for variation in abundance among regions at the start of the simulation, or losses from natural mortality before and during the period when entrainment occurs. The initial distribution of the population would have an important effect on proportional entrainment loss that arises from differences in vulnerability to entrainment among regions, and proportional entrainment loss can be biased if natural mortality is not accounted for (Kimmerer 2008). In the second stage of our modeling procedure, we use a population dynamics model, driven by unscaled movement and entrainment rates from the BMM, to estimate initial regional abundance, natural mortality rate, and salvage expansion factors. The population model predicts abundance over time in each region, as well as the number of fish from each region that are entrained, which are in turn used to compute proportional entrainment loss. Parameters of the population model are estimated via non-linear search by statistically comparing predictions of initial distribution, abundance, and salvage to field observations.

This paper focuses on the population component of the modeling framework. In particular, it examines how different assumptions about process and observation dynamics influence the fit of different BMMs to available data, and implications for PEL estimates. A companion paper describes the BMMs and predicted movement patterns in detail (Gross et al., this volume). The analysis presented in this paper largely compares predictions from the BMM and population dynamics models to observed spatial and temporal changes in catch from fish field surveys, as well as to daily salvage data from state and federal fish screening facilities. Ultimately, our objective is to better understand the strengths and limitations of available information for estimating PEL. In addition, the process of formulating hypotheses as mathematical models and fitting them to observations leads to a sharper understanding of the data, which can be invaluable for making future decisions on research and monitoring. The broader goal of the work presented here is to support a more confident assessment of Delta Smelt entrainment and, stemming from that greater understanding, to assess the efficacy of management actions used to operate the water projects in a manner consistent with the Endangered Species Act.

METHODS

Model Overview

We developed a modeling framework that consists of a behavior and particle-tracking simulation that predicts movement of adult Delta Smelt among 15 regions in the Delta (Figure 1), and a population model that estimates abundance and entrainment, given movement predictions (Figure 2). The population model estimates abundance by region, survival rate, and entrainment of adult Delta Smelt on a daily time-step, by jointly fitting to three different data sources, which include the Fall Midwater Trawl (FWMT) and Spring Kodiak Trawl (SKT) surveys, and the daily salvage estimates at state and federal fish screening facilities. The modeling framework was applied in water year 2002 for a 134-day period from December 5, 2001 to April 17, 2002. This simulation window was selected to begin just before the first flush (Grimaldo et al. 2009) and extend through most of the spawning period to the typical date when the April SKT survey is complete. Water year 2002 was selected in part because survey catches and salvage were higher than in many other years, which supports a more informed evaluation of the relative fits of different behavior and population models. In addition, water year 2002 was classified as a "Dry" water year type for both the Sacramento and San Joaquin valleys. This resulted in low Delta outflow and negative OMR flows (see Figures 3 and 6 of Gross et al., this volume) when entrainment loss is expected to be higher compared to a wetter year (Grimaldo et al. 2009 and this volume), a logical condition under which to test the models. The fit of the model to additional water years is presented in Gross et al. (2018).

The California Department of Fish and Wildlife (CDFW) FMWT survey samples 122 stations monthly from September through December,

https://doi.org/10.15447/sfews.2021v19iss1art1

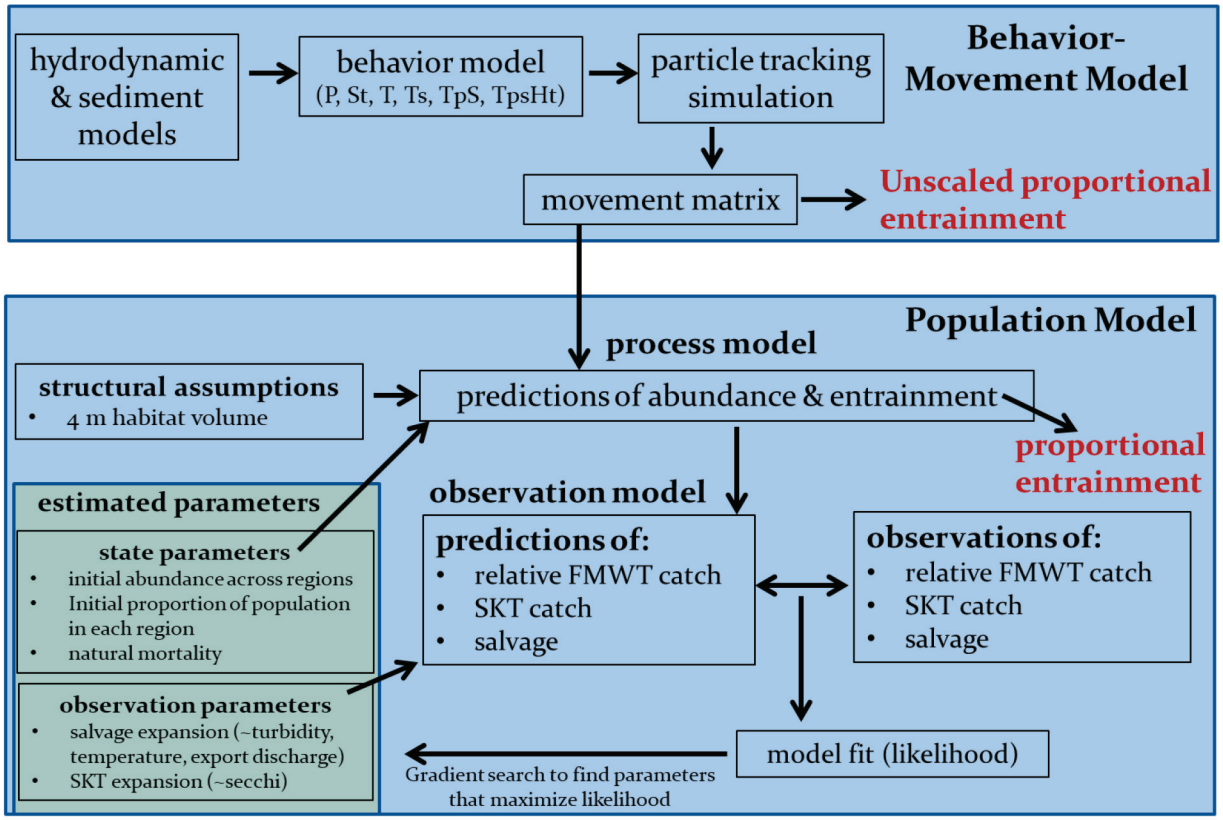

Figure 2 Overview of modeling framework used to predict movement, abundance, and entrainment of adult Delta Smelt. Note that fitting only influences parameters in the population dynamics model. Behavior-driven model parameters used in the movement model, which determine movement patterns, are treated as fixed values in the population model.

throughout the San Francisco Estuary. In this analysis, the FMWT data are compared to the predicted relative differences in abundance among regions at the start of the simulation period. The CDFW initiated the SKT in 2002 to provide a more effective means to monitor the distribution and reproductive status of Delta Smelt (IEP MAST 2015). The SKT survey samples 40 stations distributed across the Delta in monthly surveys from January through May. These observations are compared to estimated catches from the population model that depend on predictions of abundance. Fish screening facilities for state and federal pumps accumulate fish in holding tanks during sampling periods that are most often 2 hours (Kimmerer 2008). During each sampling period, a sub-sample is taken over a shorter time-period (typically 20 minutes at the state facility and 10 minutes at the federal facility), and these observations are scaled-up to daily estimates of salvage. In this analysis, daily salvage estimates are compared to estimates from the model, which depend on predictions of entrainment and salvage expansion factors.

A detailed description of the BMM is provided in a companion manuscript (Gross et al., this volume). In short, it uses three-dimensional (3-D) hydrodynamic and sediment transport models to predict depth, velocity, salinity, and turbidity fields (Figure 2). A 3-D particle-tracking model, with rules that simulate fish movement behavior, is used to predict the movement of adult Delta Smelt among 15 regions, and the proportion of particles from each region that are entrained at the CVP and SWP pumping facilities (Figure 1). The spatial resolution of the model is relatively fine near the pumps, and separately tracks the number of particles in the Clifton Court Forebay (CCF) as well as those entrained at the

SWP. Movement predictions from the BMM are summarized in a movement array which specifies the proportion of particles from each source region that remain in that region, move to other regions, or are entrained at the pumps, for each simulated day. We refer to the movement array produced from the BMM simulation as "unscaled" because it does not account for differences in the abundance of Delta Smelt among regions at the start of the simulation, or for losses from natural mortality. These effects are accounted for in the population dynamics component of the model.

The BMM is initialized by placing a large number of uniformly distributed particles in each of the 15 modeled regions. To account for particles that move outside the 15-region model domain, additional regions are defined, and the CCF location is also explicitly modeled. Rules that specify the movement behavior of each particle in response to hydrodynamic, salinity, and turbidity fields determine the location of each particle through the simulation. There is no stochastic variation in behavioral rules for individual particles, so each particle will have the same response if exposed to the same sequence of stimuli. BMMs presented here and in the companion paper (Gross et al., this volume) are a small subset of the ones we examined, but span a range of complexity. These include simple behaviors such as passive drift (no swimming behavior, model P) and swimming toward more turbid water (model St), to more complex ones such as tidal migration (model T, lateral tidal migration concept in Feyrer et al. 2013), to even more complex behaviors that are based on multiple physical cues with different thresholds or acclimatization periods (models Ts, Tps, and TpsHt; see Table 2 of Gross et al., this volume). As shown below, the TpsHt model fits the data best. This model included a tidal-migration behavior driven by perceived changes in salinity, and movement toward shallow water during ebb tide when turbidity is >12 NTU and local depth is greater than 4 m.

The population dynamics model consists of process, observation, and likelihood (fitting) components (Figure 2). The process component predicts the abundance of the population in each of 15 regions for each day of the simulation. The model uses estimates of abundance in each region and the proportion of particles in that region that are entrained, as determined by the BMM, to predict the total number of particles entrained each day. The observation component of the model translates predictions into expected catches in FMWT and SKT surveys on the days those surveys were conducted, and daily salvage at each fish screening facility. The likelihood component compares these predictions to observations. Process and observation parameters are estimated by maximizing the likelihood using a gradient search method. A total of 30 combinations of six behavior models and five population-dynamic models were fit to the data.

In the observation component of the population model, predictions of abundance and entrainment from the process component of the population model are translated into relative differences in FMWT catch at the start of the simulation, SKT catch by region and survey date, and daily salvage at each screening facility. In the fitting component of the model, these predictions are compared to data. In the description of the population dynamics model which follows, *Greek letters* denote parameters that are estimated, *upper-case letters* denote state variables (values that are predicted), and *lower-case letters* denote indices (*not bold*), or data (*bold*) or fixed parameters (*bold*).

The combined BMM and population models make a number of critical assumptions:

1. Particles released in any of the 15 regions can be potentially entrained.

2. Delta Smelt behavior does not vary over the simulation period.

3. Movement behaviors apply to all adult Delta Smelt (i.e., there is no resident component that does not move).

4. Variation in Delta Smelt abundance does not influence movement behavior.

https://doi.org/10.15447/sfews.2021v19iss1art1

5. Climate-driven effects are fully accounted for by their influence on flow, water temperature, and turbidity, which drive movement predictions.

6. Survival rate of adult Delta Smelt is constant over the modeled period or can vary temporally as a function of water temperature or model day.

7. There is no variability in survival rates among regions, though salvage efficiency implicitly models the effect of lower survival rates in central and southern regions of the Delta.

More detail on these assumptions is provided in the model description which follows, and in the Discussion.

Process Model (Population and Entrainment Dynamics)

The process component of the population-dynamics model predicts the abundance of Delta Smelt adults by model day and region. Initial abundance is calculated from

$$N_{i,d=0} = e^{\gamma} \cdot \theta_{I_i}, \quad (1)$$

where $N_{i,d=0}$ is initial abundance in each region i at the beginning of the first day of the simulation (d=0), γ is the estimated initial total abundance across all 15 regions in log-space, and θ_{I_i} is the initial proportion of the total population in each region i at the start of the simulation.

Regional abundance on subsequent days depends on cumulative survival and movement, and is calculated from

$$N_{i,d} = \Sigma_{\boldsymbol{j}} \left[N_{j,d=0} \cdot \Pi_d \phi_d \cdot \boldsymbol{m}_{\boldsymbol{j,i,d}} \right], \quad (2)$$

where ϕ_d is the estimated survival rate on day d with the product of those rates (denoted by the $\prod$ symbol) equivalent to cumulative survival to the end of day d, and $\boldsymbol{m}_{\boldsymbol{j,i,d}}$ is the cumulative proportion of fish that move from one region (j) to another (i), remain in the same region ($j=i$), or are entrained (the movement array calculated in the BMM).

Note that abundance in region i is the sum of surviving fish from source regions j that move to region i, as well as surviving fish that remain in region i between time-steps.

We do not allow the natural survival rate to vary across regions because it would require tracking the fate of tens of thousands of particles in the population model, increasing computational time by about four orders of magnitude. As reviewed in the Discussion, the limited number of SKT survey sites combined with high variation in catches among sites within regions, makes these data too un-informative to estimate regional variation in survival rate. However, as discussed below, additional mortality for particles that are entrained, which must pass through the South Delta, is captured in the estimate of the salvage expansion factor.

Two formulations of natural survival rate are used to predict potential temporal variation. The simplest assumption is that survival is constant over time (survival model S_c) and is therefore calculated as

$$\phi_d = \text{logit}\left(\alpha_0\right), \quad (3A)$$

where α_o is an estimated survival rate in logit space. The logit() term denotes that the value inside the parentheses is logit-transformed, so $0 \le \phi_d \le 1$.

Alternatively, we assume that daily survival rate over time can vary as a logistic function of model day (survival model S_d) using

$$\phi_d = \text{logit}\left(\alpha_0 + \alpha_1 \cdot d\right), \quad (3B)$$

A negative value of α_1 will lead to declining survival rate over time, which may occur as a result of spawning-related mortality because

the majority of individuals in any year are semelparous (Moyle et al. 2016; Bennet 2005).

The cumulative number of fish entrained is calculated from

$$N\_Ent_{k,d} = \Sigma_d \Sigma_i \left[N_{i,d=0} \cdot \Pi_d \phi_d \cdot \left(\boldsymbol{m}_{i,k,d} - \boldsymbol{m}_{i,k,d-1} \right) \right], \quad (4)$$

where N_Ent is the number entrained at fish screening facility k ($k = 1$ or 2) from the start of the simulation through day d, and $\boldsymbol{m_{i,k,d}}$ is the cumulative proportion of fish from source region i that are entrained at location k, as determined by the BMM. Equation 4 scales the proportional entrainment rates from the BMM by accounting for differences in initial abundance among regions and losses from natural mortality.

The proportion of the initial population that is entrained at each fish screening facility up to and including day d is calculated from

$$p\_Ent_{k,d} = 1 - \Pi_d \left[1 - \frac{N\_Ent_{k,d} - N\_Ent_{k,d-1}}{\Sigma_i N_{i,d-1}} \right], \quad (5)$$

where $N\_Ent_{k,d} - N\_Ent_{k,d-1}$ represents the number of Delta Smelt entrained at fish facility k on day d, and represents the total abundance across all regions at the beginning of day d.

Equation 5 follows the same logic as Kimmerer (2008) and assumes natural and entrainment mortality are continuous processes. As a result, proportional entrainment on each day depends on the abundance at the end of the previous day, where that abundance in turn depends on the initial abundances as well as cumulative natural and entrainment losses. The term inside the product symbol ($\prod$) is the proportion of the population that survives entrainment on day d, and that product over days is the cumulative proportion that survive from the start of the simulation through day d. Thus, 1– this product is the proportion of the population that is lost to entrainment. Entrainment losses include: (1) pre-screen losses; (2) losses from the fish screens to the salvage collection facility; and (3) the number of fish that are salvaged. The third element assumes that all Delta Smelt that are salvaged will not survive after their release back into the Delta (Bennett 2005; Miller 2011).

We provide two proportional entrainment loss metrics in this analysis. We refer to the output from Equation 5 as PEL for each facility, and the sum of those PELs is the total entrainment. We also refer to an "unscaled proportional entrainment loss," which is just the output from the BMM from all source regions to each facility on the last simulation day D ($\boldsymbol{m_{i,k,D}}$). These values are the proportion of the initial particles entrained by the end of the simulation. They describe relative differences in vulnerability to entrainment among the 15 regions. The contribution of each region to the total entrainment depends on these values, but also on the initial abundance estimated for each region at the start of the simulation, and on the natural survival rate. Unscaled proportional entrainment statistics provide a simple summary to compare BMMs and are not affected by population or observation parameters.

Observation Model (Predicting SKT Catch and Salvage)

SKT Catch

The observation component of the population model predicts SKT catch for each station and survey period from

$$\hat{C}_{SKT_{s,d}} = N_{i(s),d} \cdot \theta_{SKT_{s,d}}, \quad (6A)$$

where $\hat{C}_{SKT_{s,d}}$ is the predicted SKT catch at station s on day d, $N_{i(s),d}$ is the predicted abundance in region i where station s is located ($i(s)$), and $\theta_{SKT_{s,d}}$ is the proportion of the population in region i sampled at station s on day d.

We refer to the latter term as SKT sampling catchability, and it is calculated from

$$\theta_{SKT_{s,d}} = \theta_{c_{s,d}} \frac{\mathbf{vtow}_{s,d}}{\mathbf{vreg}_i}, \quad (6B)$$

https://doi.org/10.15447/sfews.2021v19iss1art1

where $\theta_{c_{s,d}}$ is an estimate of the proportion of Delta Smelt that are captured within the volume towed at a station (sampling efficiency), $\mathbf{vreg_i}$ is the volume of region i that Delta Smelt are distributed in, and $\mathbf{vtow_{s,d}}$ is the volume for the tow at station s in region i sampled on day d.

We assumed that Delta Smelt were evenly distributed to a maximum depth of 4 m (as in Kimmerer 2008). Assumptions about the depth distribution of Delta Smelt have no effect on our estimates of PEL because they are accounted for in the estimates of salvage expansion factors. For example, if the maximum depth is set to 2 m, the predicted abundance of the population will be lower than if estimated based on a maximum depth of 4 m. However, as shown below, to match the observed salvage data, the salvage expansion under the 2-m depth distribution will be higher than under the 4-m distribution. The proportion of Delta Smelt within the volume towed that is captured can either be set to 1 or calculated from

$$\theta_{c_{s,d}} = \text{logit}\left(\beta_0 + \beta_1 \cdot \mathbf{secchi}_{s,d}\right), \quad (6C)$$

where β_0 and β_1 are parameters that predict SKT sampling efficiency as a function of Secchi disc depth recorded at each station on each SKT survey.

Delta Smelt may be able to avoid capture to a greater extent when the water is clear, which would result in a negative estimate for β_1 (Latour 2016). Increased water clarity may also result in a change in the vertical or lateral distribution of Delta Smelt, which could also affect sampling efficiency because the SKT samples the top 2 m of the water column, and typically well away from the shorelines. Other factors that could affect sampling efficiency could also be modeled using the format in Equation 6C, but were not explored in this paper for brevity and because of lack of evidence for them. Catchability, the proportion of the population in a region captured at a station, is the product of θ_c and the constants $\mathbf{vtow_{s,d}}/\mathbf{vreg_i}$ (Equation 6B). Station- and survey-specific effects on catchability (θ_c) are easily excluded by not estimating parameters that define $\theta_{c_{s,d}}$ and instead fixing this value at 1. In this case, catchability for any region is simply the ratio of the volume sampled in that region across stations on a particular survey to the volume over which Delta Smelt are assumed to be distributed. Owing to the very large volumes of each region, the proportion of the population sampled on each survey is very small (Table 1). Because of spatial variation in Delta Smelt densities within a region and the small proportion of total habitat that is sampled, the average density taken over a series of tows within an individual region may be very different than the actual mean density for the region.

Salvage

Salvage in the observation component of the population dynamics model is calculated from

$$\hat{C}_{SAL_{k,d}} = \left(N\_Ent_{k,d} - N\_Ent_{k,d-1}\right) \cdot \theta_{S_{k,d}} \cdot \mathbf{p_{s_k}}, \quad (7)$$

where $\hat{C}_{SAL_{k,d}}$ is the predicted salvage on model day d at fish screening facility k, is the proportion of entrained fish that are salvaged, and $\mathbf{p_{s_k}}$ is the proportion of the daily volume of exported water that is sampled for fish.

For consistency with past efforts, we calculate the salvage expansion factor, which is simply the inverse of salvage efficiency (θ_S^{-1}). Time-specific values for $\mathbf{p_S}$ for each facility were not available for the entire simulation period. The "observed" daily salvage data available to us were already expanded to account for the proportion of volume sampled each day. By using expanded salvage observations, one is assuming that $\mathbf{p_S} = 1$. However, when fitting the model, using expanded salvage data would inflate the importance of the salvage data relative to other data sources (FMWT, SKT). To correct for this, $\mathbf{p_S}$ was set to values that reflected the typical proportion of flow at each salvage facility that was sampled for fish. We set $\mathbf{p_S}$ to 0.08 (sampling 10 minutes out of every 2 hours) for the Tracy Fish Collection Facility at the CVP, and 0.18 (sampling 21.6 minutes every 2 hours) at the Skinner Fish Facility at the SWP, which were the averages

Table 1 Region-specific, volume-based, sampling expansions applied to the Spring Kodiak Trawl (SKT) data to estimate Delta Smelt abundance (θ_{SKT}), and unscaled estimates of proportional entrainment loss (PEL) of Delta Smelt (*colored columns*) in water year 2002. SKT expansion factors, used to convert regional abundance estimates (*N*) to catch ($c = N \cdot \theta_{SKT}$), are based on the ratio of the volume towed to habitat volume over which adult Delta Smelt are assumed to be distributed. Unscaled PEL, as predicted by six behavior-driven movement models (BMM), represents the proportion of particles released in each region that are entrained at either the federal or state pumping facilities. The "Total or Average" row shows the average SKT expansion factor across regions, and for PEL is the sum product of the proportion of the initial population in each region (based on volume-adjusted FMWT catch) and the region-specific unscaled PEL values. The "PEL" row shows the most likely proportional entrainment loss estimate for each BMM based on fitting population dynamics model 5 (see Table 2). The "SFbay" row is the FMWT-weighted proportion of particles from each source region that enters the San Francisco Bay ghost region. Behavior models include passive (P); turbidity seeking (St); lateral tidal migration (T); tidal migration when salinity > 1 psu (Ts); tidal migration when perceived salinity is increasing (Tps); and as for Tps but with holding behavior when turbidity > 12 NTUs (TpsHt).

				Behavior model					
Region Name	**Region abbreviation**	**Location**	θ_{SKT}^{-1}	**P**	**St**	**T**	**Ts**	**Tps**	**TpsHt**
Napa River	napa	West	4,570	0.00	0.00	0.11	0.02	0.05	0.05
Carquinez Strait	carq	West	13,986	0.00	0.00	0.58	0.03	0.03	0.05
West Suisun Bay	wsuisb	West	6,591	0.00	0.00	0.60	0.03	0.07	0.14
Mid Suisun Bay	msuisb	West	8,429	0.00	0.00	0.58	0.03	0.12	0.22
Suisun Marsh	smarsh	West	1,617	0.00	0.00	0.03	0.00	0.11	0.12
Chipps Island	chipps	West	5,078	0.00	0.00	0.64	0.04	0.16	0.30
Sacramento River near Sherman Lake	sac_sherm	Central	4,452	0.00	0.00	0.58	0.04	0.20	0.41
Sacramento River near Rio Vista	sac_rio	North	3,965	0.10	0.03	0.45	0.12	0.34	0.57
Cache Slough and SDWSC	cache_dwsc	North	4,188	0.05	0.03	0.07	0.06	0.22	0.30
Sacramento River and Steamboat Slough	sac_steam	North	1,822	0.36	0.23	0.12	0.37	0.53	0.61
San Joaquin River near Antioch	sjr_ant	South	3,874	0.08	0.07	0.74	0.10	0.23	0.48
Central Delta and Franks Tract	cdelta	South	5,526	0.77	0.58	0.65	0.75	0.80	0.90
North and South Forks Mokelumne River	mok	East	1,518	0.87	0.83	0.13	0.88	0.88	0.89
San Joaquin near Stockton	sjr_stk	East	3,697	0.98	0.78	0.13	0.98	0.98	0.98
South Delta	sdelta	South	5,283	0.99	0.97	0.98	0.99	0.99	0.99
		Total or Average	4,973	0.04	0.02	0.44	0.07	0.24	0.42
		PEL		0.02	0.05	0.38	0.06	0.19	0.35
		SFbay		0.91	0.55	0.00	0.02	0.08	0.01

https://doi.org/10.15447/sfews.2021v19iss1art1

from available data for water year 2002 during the simulation period.

The simplest model of salvage efficiency ($\theta_{S_{k,d}}$) assumes it can vary across facilities but does not vary over time:

$$\theta_{S_{k,s}} = \text{logit}\left(\lambda_{0_k}\right) \cdot \boldsymbol{FE}_{\boldsymbol{k,d}}\,, \qquad (8A)$$

where λ_0 is the proportion of entrained fish that will be captured at facility k on day d (in logit space) after accounting for daily variation in facility efficiency (***FE***).

FE values were estimated based on water velocities at the intake structures by Smith (2019) and are treated as fixed values in this analysis. The average FEs over the modeled period at CVP and SWP were 0.18 (SD = 0.05) and 0.23 (SD = 0.07), respectively.

Alternate models allow salvage efficiency to vary over time as a function of covariates using

$$\theta_{S_{k,s}} = \text{logit}\left(\lambda_{0_k} + \lambda_{1k} \cdot \boldsymbol{X}_{\boldsymbol{k,d}}\right) \cdot \boldsymbol{FE}_{\boldsymbol{k,d}}\,, \qquad (8B)$$

where λ_0 is the proportion of entrained fish that enter the facility when the covariate $\mathbf{X}$ is 0, and λ_{1k} is a linear effect of the covariate $\mathbf{X_{k,d}}$, which varies over time and can vary across facilities.

This model is easily extended to include multiple covariates by simply including additional additive effects (i.e., additional $\lambda_{1k} \cdot \mathbf{X_{k,d}}$ terms). The covariates we explored that might affect the magnitude of $\theta_{S_{k,d}}$ were: daily averaged export flow (pumping) rates for each facility (as calculated by the DAYFLOW model; CDWR 2019); water clarity, as indexed by turbidity measured just outside the entrance gates to CCF; and water temperature as measured at Mallard Island (Figure 1). Missing CCF turbidity measurements from December 13-30, 2001; January 24-30, 2002; and March 20-22, 2002 were replaced with estimates calculated from a CCF turbidity-Vernalis suspended-sediment-concentration relationship as used in Grimaldo et al. (this volume).

Because our model accounts for the effect of intake water velocity on facility efficiency, covariates that determine salvage efficiency largely represent effects on pre-screen loss, which is defined here as the proportion of entrained fish eaten by predators between the point they are entrained and the point when they reach the fish screens. Covariate effects could also account for variation in facility efficiency not accounted for by intake velocity. Turbidity could affect the reaction of fish to the louvers and thus the efficiencies of the screens. Turbidity could also affect the ability of visual sight predators such as Striped Bass or Largemouth Bass to detect and consume Delta Smelt that are eventually entrained, or how Delta Smelt behave when they are vulnerable to predation. As an example, if higher turbidity reduces predation and hence pre-screen losses, salvage efficiency should increase (and thus λ_1 should be positive). Water temperature would change the activity level of Delta Smelt and predators through effects on metabolism and behavior, which would influence which would influence the susceptibility of Delta Smelt to entrainment and predation.

Model Fit (Comparing Model Predictions to Observations)

The model is fit to the data by minimizing a total negative log likelihood (NLL_{TOT}) that quantifies the combined fit of the model to FMWT catch (NLL_{FMWT}), SKT catch (NLL_{SKT}), and salvage data (NLL_{SAL}). The total negative log likelihood is computed from

$$NLL_{TOT} = NLL_{FMWT} + NLL_{SKT} + NLL_{SAL}\,. \qquad (9)$$

Each likelihood component is described below. Note that the total negative log likelihood only quantifies the discrepancy between predictions and observations (observation error). There is no component that penalizes process variation in population-dynamic processes such as survival rates, because that variation is not modeled. In data-limited situations it is not possible to

separate process error from observation error. Including both would increase computational time considerably, and would require informative priors on the extent of process or observation error, with total variance estimates conditional on those priors. Furthermore, because we treat behavioral parameters as constants in our two-stage modeling procedure, it is not possible to include process error in parameters that influence movement. We therefore use an "observation error only" model (see Ahrestani et al. 2013), which will result in an under-estimation of uncertainty in model predictions.

It is widely acknowledged that the FMWT program does not provide a sensitive index of Delta Smelt abundance, and that the survey has an unknown capture probability (Polansky et al. 2019). In this modeling effort, we assume only that the FMWT catch provides a reliable index of relative differences in abundance across the 15 regions at the start of the simulation in early winter. After correcting for differences in sampling effort in each region (the proportion of the volume that is sampled relative to the volume over which Delta Smelt are distributed), the total FMWT catch of Delta Smelt in each region summed across the four surveys between September and December can be thought of as a random variable drawn from a multinomial distribution:

$$NLL_{FMWT} = -\sum_{i} \log\left(multinom\left(\mathbf{c}_{\mathbf{FMWT_i}}, \theta_{I_i} \right) \right), \quad (10)$$

where NLL_{FMWT} is the sum of negative log likelihood values from a multinomial distribution (see Appendix A, section A1.1) across the 15 regions, with observed volume-adjusted catches $\mathbf{c}_{\mathbf{FMWT}}$, and initial regional proportions defined by model-estimated θ_{I_i} values in Equation 1 (the proportion of the initial population in each region at the start of the simulation). In the absence of any other information, this error structure will result in a set of estimated initial proportions equivalent to the ratio of each region's volume-adjusted catch relative to the total volume-adjusted catch (see Appendix A, section A1.2).

We assume that the SKT surveys provide a comparatively reliable index of abundance across regions and over SKT survey periods in a year (Polansky et al. 2019). Unlike the FMWT likelihood, we assume that the capture probability of the SKT survey is known, and is accurately determined by the scaling factors in Equation 6A. SKT catch at each station and SKT survey period is assumed to be a random variable drawn from a negative binomial distribution (negbin):

$$NLL_{SKT} = -\sum_{s,d} \log\left(negbin\left(\mathbf{c}_{\mathbf{SKT_{s,d}}}, \hat{C}_{SKT_{s,d}}, \tau \right) \right), \quad (11)$$

where NLL_{SKT} is the sum of negative log likelihoods across all sampling days (d) and stations (s), $\mathbf{c}_{\mathbf{SKT_{s,d}}}$ is the observed SKT catch by station and day, $\hat{C}_{SKT_{s,d}}$ is the predicted catch from Equation 6A, and τ represents the extent of over-dispersion in the data. In this form of the negative binomial, the latter parameter is the variance-to-mean ratio and reflects the average extent of variation in catches across stations within regions and surveys. We refer to this as the SKT sampling error (see Appendix A, section A1.3). The value of τ for water year 2002 (Equation 11) was estimated by fixing the density on each SKT survey and region at its conditional maximum likelihood value (sum of catches across stations divided by sum of tow volumes). A value of $\tau = 10$ was used when we fit parameters of the population-dynamics model. Greater belief in the SKT data would be simulated by lowering τ. At a minimum value of $\tau = 1$, the negative binomial distribution is

https://doi.org/10.15447/sfews.2021v19iss1art1

equivalent to the Poisson, where the variance is equal to the mean.

The observed salvage at each salvage location is assumed to be a Poisson-distributed (*pois*) random variable (see Appendix A, Section A1.4):

$$NLL_{SAL} = -\sum_{k,d} \log\left(pois\left(\mathbf{c}_{\mathbf{SAL_{k,d}}} \cdot \mathbf{p}_{\mathbf{S_k}}, \hat{C}_{SAL_{k,d}} \right) \right), \quad (12)$$

where NLL_{SAL} is the sum of the negative log likelihoods across all days, $\mathbf{c}_{\mathbf{SAL_{k,d}}}$ is the reported expanded daily salvage at facility k on day d, $\mathbf{p}_{\mathbf{S_k}}$ is the average proportion of water that is sampled for fish at the screening facility, and $\hat{C}_{SAL_{k,d}}$ is the predicted salvage computed from Equation 7. By including the proportion of water sampled for fish at the screening facilities for both observations (Equation 12) and predictions (Equation 7), correct samples sizes are used in the likelihood.

Parameters of the model were estimated by maximum likelihood using nonlinear search in the AD model-builder software (ADMB; Fournier et al. 2011). We ensured convergence had occurred based on the gradients of change in parameter values relative to changes in the log likelihood and the condition of the Hessian matrix returned by ADMB. Asymptotic estimates of the standard error of parameter estimates at their maximum likelihood values were computed from the Hessian matrix within ADMB and used to calculate confidence intervals.

Model Comparison

We used the Akaike Information Criteria (AIC) to compare BMMs and alternate versions of the population model. AIC measures the trade-off between model complexity and fit, and is calculated from

$$\mathrm{AIC} = 2 \cdot \mathrm{K} - 2 \cdot \mathrm{LL}, \quad (13)$$

where K is the number of estimated parameters, and LL is the log likelihood calculated as $-NLL_{TOT}$ from Equation 9. More complex models with more parameters (higher K) may fit the data better (higher LL) than simpler models, but parameter estimates will be less precise. Models with lower AIC (i.e., higher LL and lower K) are considered to have better predictive performance when applied to replicate data sets. Models within 0 to 2 AIC units of the most parsimonious model (the one with the lowest AIC) are considered to have strong support and cannot be distinguished; models within 2 to 7 units are considered to have moderate support, and models that had AIC values >7 units relative to the best model are considered to have weak support (Burnham and Anderson 2002).

Our main analysis compares five different versions of the population-dynamics model for each of the six behavior-driven movement models. The different population-dynamics models are intended to span a range of process and observation dynamics. The simplest population model we examined estimates 19 parameters, which include the total initial abundance, 15 regional initial abundance proportions, one constant salvage efficiency for each facility, and one constant survival rate. We also examine models that allow survival to vary as a logistic function of model day; for salvage efficiency to vary as a function of turbidity, temperature, and export discharge; and for SKT sampling efficiency to vary as a function of Secchi depth.

RESULTS

The proportion of particles released in each region that were entrained in pumping facilities was highly variable across BMMs (Table 1). With the exception of the tidal migration behavior model (BMM T), unscaled PEL values were generally greater than 0.8 in southern and eastern regions (cdelta, mok, sjr_stk, and sdelta). Passive (P), turbidity-seeking (St), and tidal-salinity (Ts) BMMs had low unscaled PEL for most western and northern regions because particles either moved rapidly to sea or far inland—patterns which fit the spatial and temporal trend in the SKT data poorly (see Table 2). The tidal migration

Table 2 Comparison of six behavior-driven movement models (BMMs, *rows*) and five population- dynamic model structures (*columns*). For the population models, salvage efficiency was assumed to be constant over time (const) or vary as a function of turbidity (~turb). Natural survival rate was assumed to be constant over time (S_c) or vary as a function of model day (S_d). Spring Kodiak Trawl (SKT) sampling efficiency was either assumed to be constant (const) or vary as a function of Secchi disc depth (~Secchi). The ΔAIC rows show the difference between each model's AIC relative to the model with the lowest AIC (and thus, the model with ΔAIC = 0 has the lowest AIC and is considered the best model). The model rank rows show the rank of each BMM within each population model type as determined by AIC (rank 1 = best model). Proportional entrainment loss rows show the maximum likelihood estimate of the total proportional entrainment loss across federal and state facilities. The SWP salvage expansion rows show the salvage-weighted average salvage expansion factor over the simulation at the state facility. See caption for Table 1 for BMM definitions.

Population model	**1**	**2**	**3**	**4**	**5**
Salvage efficiency	**const**	**const**	**const**	**~turb**	**~turb**
Natural survival rate	**S_c**	**S_d**	**S_d**	**S_c**	**S**
SKT efficiency	**const**	**const**	**~Secchi**	**const**	**const**
Number of population parameters	19	20	22	21	22
ΔAIC					
passive (P)	777	770	769	504	495
turbidity seeking (St)	5,092	5,079	5,014	4,781	4,742
tmd (T)	2,916	2,901	2,851	1,778	1,765
ptmd_sal_gt_1 (Ts)	767	560	564	422	296
ptmd_si_pt_5 (Tps)	667	434	437	360	171
ptmd_si_pt_5_shallow_ebb_t_gt_12 (TpsHt)	485	360	357	102	0
Model Rank					
passive (P)	4	4	4	4	4
turbidity seeking (St)	6	6	6	6	6
tmd (T)	5	5	5	5	5
ptmd_sal_gt_1 (Ts)	3	3	3	3	3
ptmd_si_pt_5 (Tps)	2	2	2	2	2
ptmd_si_pt_5_shallow_ebb_t_gt_12 (TpsHt)	1	1	1	1	1
Proportional Entrainment Loss					
passive (P)	0.02	0.02	0.02	0.02	0.02
turbidity seeking (St)	0.02	0.02	0.02	0.05	0.05
tmd (T)	0.39	0.39	0.40	0.38	0.38
ptmd_sal_gt_1 (Ts)	0.06	0.06	0.06	0.06	0.06
ptmd_si_pt_5 (Tps)	0.19	0.18	0.18	0.20	0.19
ptmd_si_pt_5_shallow_ebb_t_gt_12 (TpsHt)	0.35	0.34	0.34	0.36	0.35
SWP Salvage Expansion Factor					
passive (P)	73	73	95	76	76
turbidity seeking (St)	9	9	68	35	35
tmd (T)	58	56	114	142	139
ptmd_sal_gt_1 (Ts)	12	11	373	16	15
ptmd_si_pt_5 (Tps)	48	40	925	60	47
ptmd_si_pt_5_shallow_ebb_t_gt_12 (TpsHt)	111	102	120	140	127

https://doi.org/10.15447/sfews.2021v19iss1art1

BMM (T) resulted in rapid inland dispersal, which led to high values of PEL in many central and western regions, and lower values in the most eastern regions. The most complex BMMs (TpS, TpsHt), which fit the data best (see Table 2), generally showed higher unscaled PEL values for regions that were closer to the pumps. We calculated an across-source region (integrated) unscaled PEL value by multiplying region-specific PEL values by the initial proportion of the population in each source region as determined by the FMWT data only. The top-ranked BMM (TpsHt) had an integrated unscaled PEL ("Total or Average" row of Table 1) of 0.42. The best estimates of PEL for each BMM, as determined from the top-ranked population model (PEL row in Table 1) were, on average, 15% lower than the across-region unscaled values, but the two types of PEL estimates were highly correlated ($r^2 = 0.99$). This demonstrates that predictions of movement from the BMMs are the dominant driver of PEL estimates in the population model.

The most complex BMM we evaluated (TpsHt), combined with a population model that included daily variation in natural survival rate, as well as turbidity-driven salvage expansion (population model 5), had the lowest AIC value of all 30 model combinations (Table 2). This top-ranked model provided a very good fit to the volume-adjusted FMWT catch data summed across the September, October, November, and December surveys ($r^2 = 0.98$; Figure 3 *top-left panel*). The predicted abundances (Figure 3, *top-right panel*) describe the distribution of the population among regions at the start of the simulation on December 5, 2001. The model predicted an initial abundance of about 1.9 million fish across all regions at the start of the simulation, with a 95% credible interval of 1.5 to 2.3 million. The model predicted a substantial decrease in daily survival rates after late February (Figure 3, *lower-left panel*), consistent with the understanding that most Delta Smelt are semelparous and die after spawning (Bennet 2005). The predicted total abundance of the population across regions was somewhat close to values calculated from expanding the SKT catch data by the ratio of regional 4-m volume-to-tow ratio on the last two surveys (Table 1). The model substantially over-predicted abundance on the January survey (Figure 3, *lower-right panel*) because its structure dictates that abundance must decline over the course of the simulation, which was not consistent with the higher data-predicted abundance on the February SKT survey compared to the January survey.

The top-ranked combination of models (BMM TpsHt–population model 5, Table 2) explained 70% of the spatial and temporal variation in SKT catch based on data from all regions and trips (Figure 4). It made qualitatively correct predictions of the trends in abundance between the January, February, and March surveys for five of 15 regions (carq, chipps, sjr_ant, cdelta, and sdelta). The model did not capture what appears to be movement into Napa and Sacramento rivers and the Cache Slough deepwater ship channel between February and March surveys. The model consistently over-predicted abundance in the South Delta region by a small amount. Examination of standardized SKT catch residuals removes the effect of differences in catch rates across regions and surveys, allowing a comparison of relative differences in model fit to the SKT data (Figure 5). Standardized residual patterns show the model substantively under-predicted abundance in Suisun Marsh (smarsh) during the January, February, and March surveys and in most Sacramento River-influenced regions during the March survey. The model also tended to over-predict abundance in most western regions and central regions during the January survey. In a relative sense, the fit to the South Delta region was good on all three surveys. The model also tended to over-predict abundance in January and under-predict abundance in March. This could indicate that Delta Smelt are changing their behavioral responses to abiotic cues over time, a dynamic that is not included in the BMMs.

The top-ranked model accurately captured broad patterns in the temporal trends in daily salvage data. At the CVP, 80% of the total observed and predicted salvage had occurred by January 21, 2002 and February 6, 2002, respectively

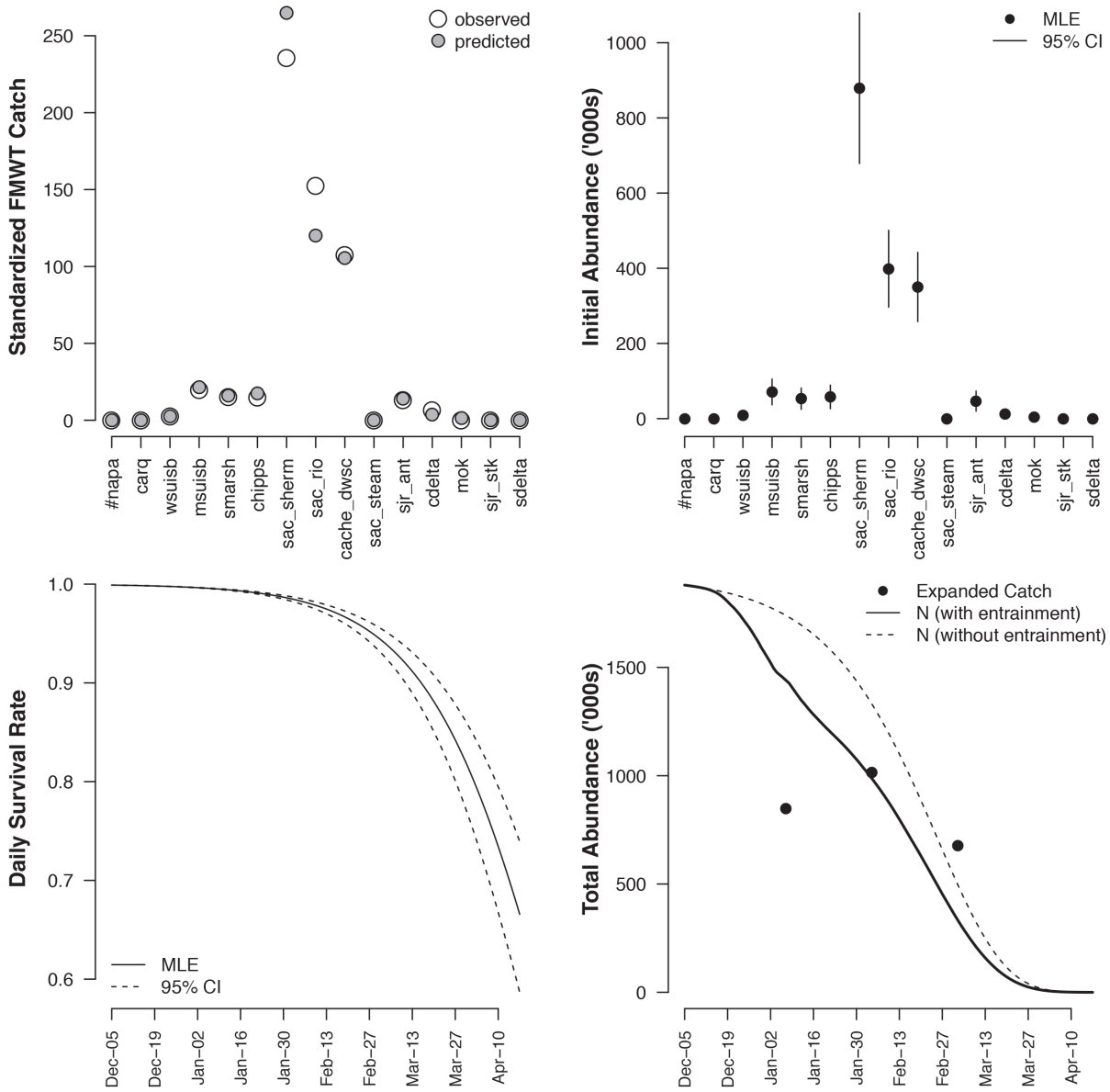

Figure 3 Model fit and predictions for the TpsHt behavior-driven model and population model 5 (see Table 2) showing: maximum likelihood estimates (MLEs) of predicted and observed volume-corrected FMWT catch (*top-left plot*, observed catch summed across Sep, Oct, Nov, and Dec. surveys); MLEs of initial population estimates by region with 95% credible intervals (*top–right plot*); MLEs of the daily survival rate (*solid line*, *bottom-left plot*) with 95% credible intervals (*dashed lines*), and the trend in predicted total abundance across regions (*bottom-right plot*, *solid and dashed lines*) compared to estimates based on expanding the catch by the ratio of regional habitat volume to the volume of tows (*points*). The predicted abundance on December 5th in the *bottom-right panel* is the sum of initial abundance estimates across regions.

(Figure 6). At the SWP, 80% of the total observed and predicted salvage occurred by January 12, 2001 for both observations and predictions. Observed salvage at the end of December increased rapidly about a week after an increase in turbidity at the CCF. The model predicted earlier and faster increases in salvage compared to the observed trends. Over the entire 134-day simulation period, the model explained 28% and 42% of daily variation in salvage at the federal

https://doi.org/10.15447/sfews.2021v19iss1art1

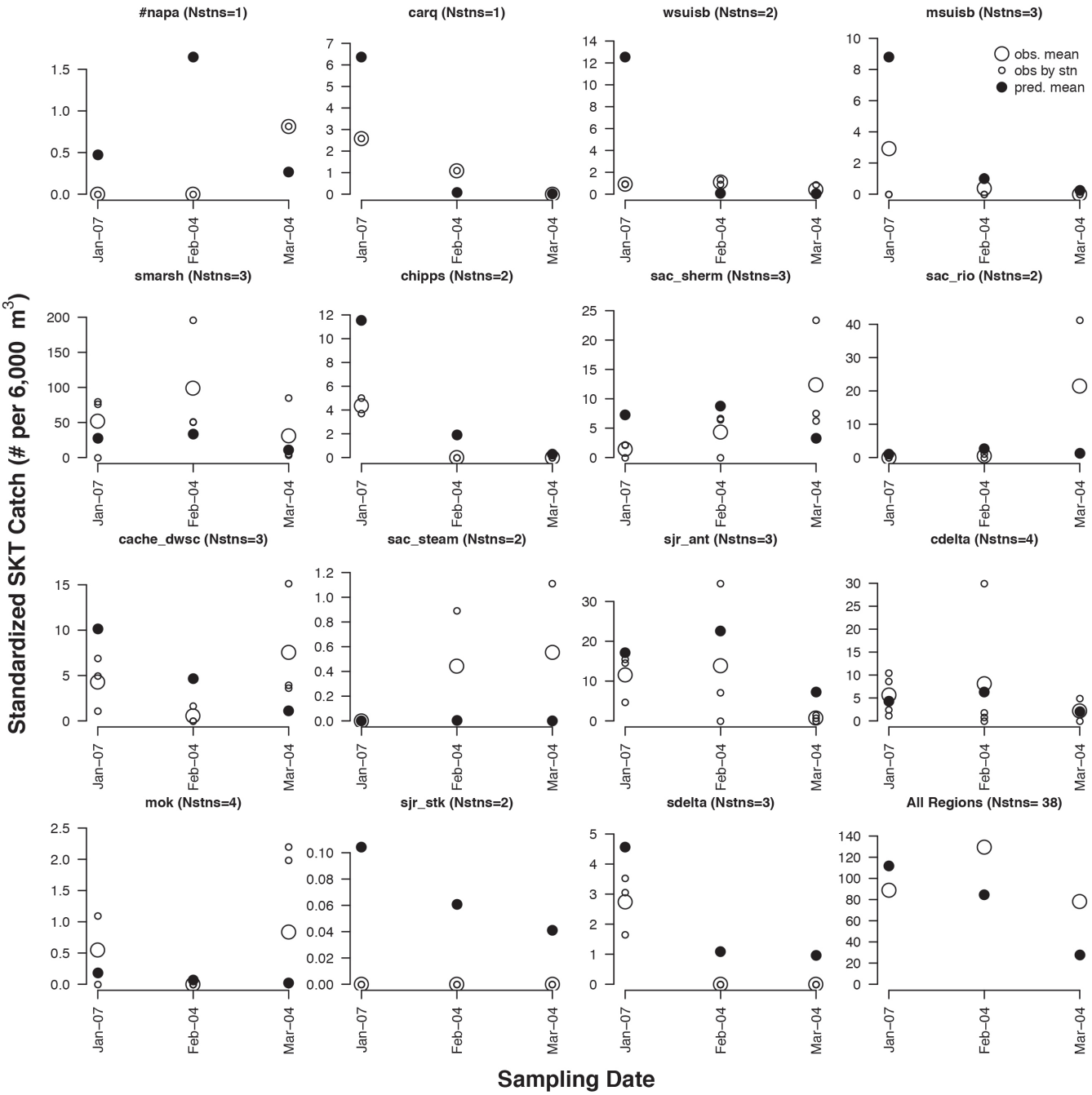

Figure 4 Comparison of predicted (*gray points*) and mean observed (*large open points*) SKT catch by trip and region, where catches are standardized by the approximate average tow volume. Also shown are the standardized station-specific catches (*small open points*). Predictions are from the TpsHt behavior model and population model 5 (see Table 2).

(CVP) and state (SWP) facilities, respectively. The model predicted that pre-screen loss decreased with increasing turbidity, and that the turbidity effect at the CVP was much weaker compared to the SWP (Figure 7). This is consistent with the observations that no salvage at SWP occurred when turbidity was less than ~15 NTUs, and that salvage occurred on all days that had a turbidity of greater than ~30 NTUs. The strong effect of turbidity at the SWP resulted in considerable

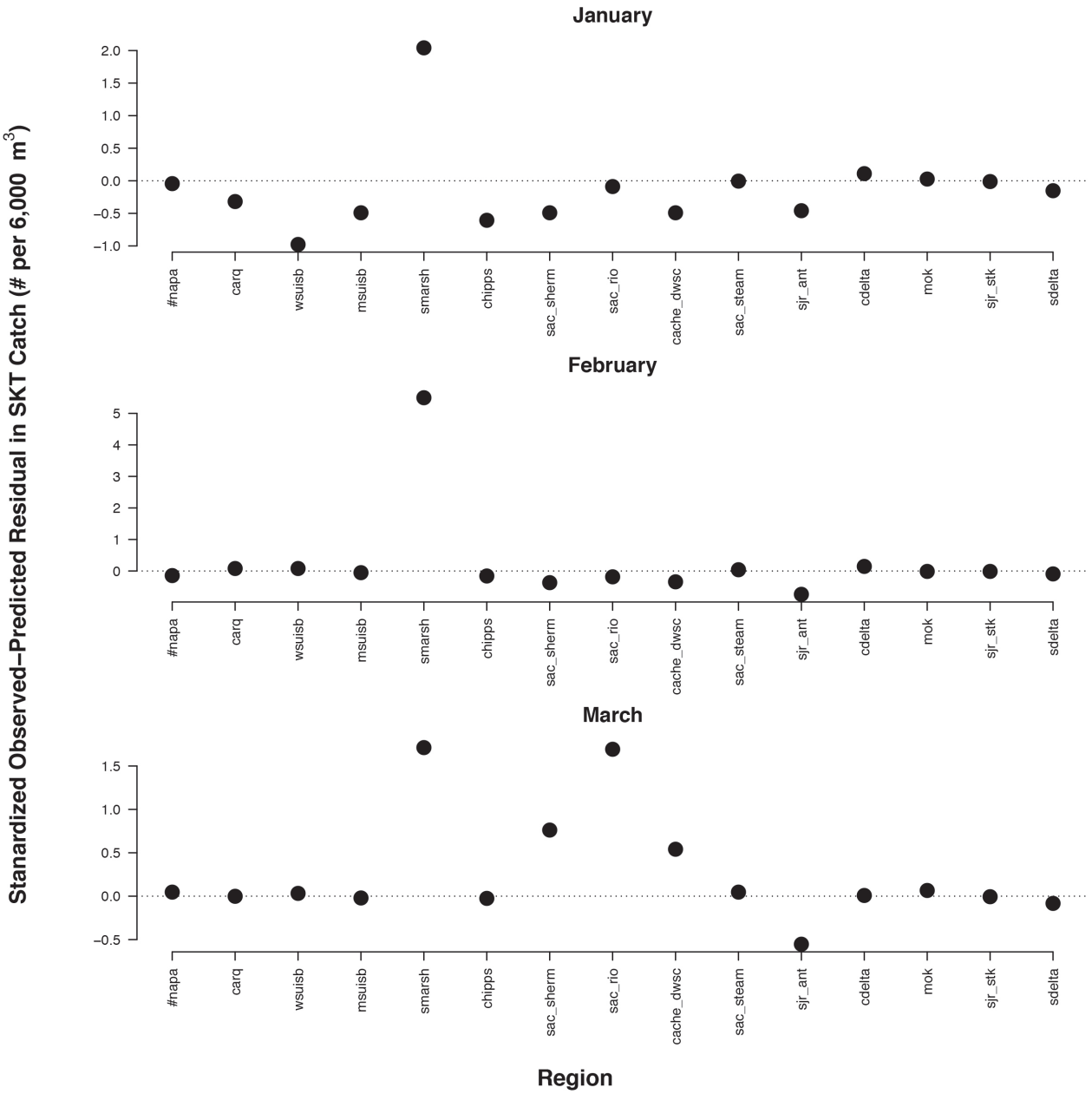

Figure 5 Standardized Spring Kodiak Trawl (SKT) residuals by region and survey. Residuals were computed based on the difference between observed and predicted SKT catch (standardized to a tow volume of 6,000 m^3) and then dividing each residual by the standard deviation of all residuals. A positive residual indicates the model is under-predicting abundance; the converse indicates over-prediction. Predictions are from the TpsHt behavior model and population model 5.

daily variation in expansion factors compared to the relatively constant pattern at the CVP (Figure 6). The observed salvage-weighted average expansion factor over the simulation period was 127 at the SWP and 74 at the CVP. These differences between facilities could reflect higher levels of pre-screen loss in the CCF at the SWP (Castillo et al. 2012). Allowing the salvage expansion factor to vary with turbidity resulted in a better fit to the salvage data, especially at the SWP. Because the majority of the salvage expansion is determined by pre-screen loss—

https://doi.org/10.15447/sfews.2021v19iss1art1

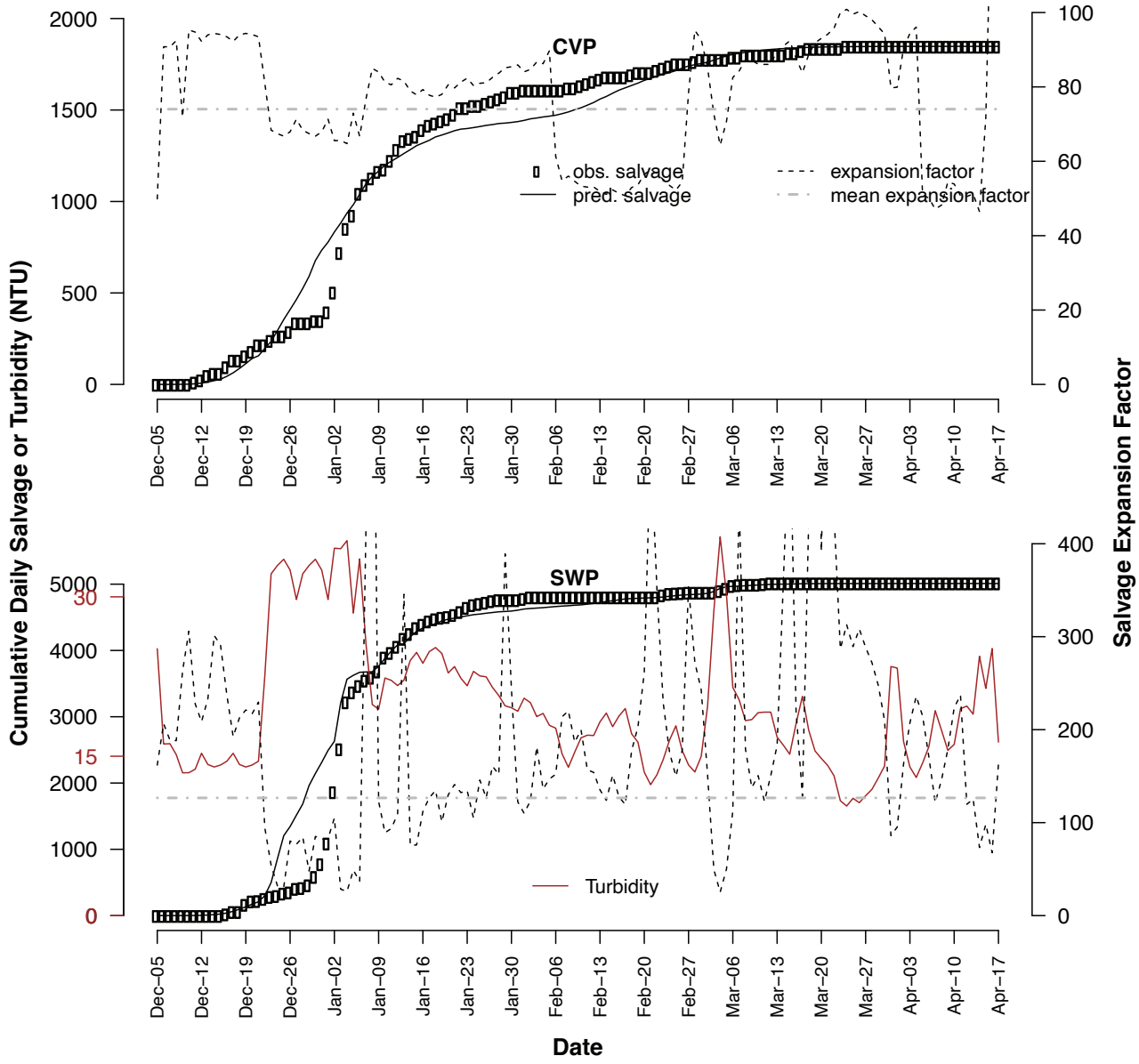

Figure 6 Predicted (*solid black line*) and observed (*points*) cumulative daily salvage (*left axis*) at federal (CVP) and state (SWP) fish-screening facilities. Also shown are the estimated daily salvage expansion factors ($1/\theta_S$, *black dashed line*, *right-hand axis*), which depend on turbidity, the salvage-weighted average salvage expansion factor across days (*horizontal dashed line*), and turbidity in the Clifton Court Forebay (CCF, *brown line*, and *brown y-axis labels on left axis*). Predictions are from the TpsHt behavior model and population model 5 (see Table 2).

at least at the SWP where facility efficiency and pre-screen loss have both been measured by mark-recapture (Castillo et al. 2012)—this result suggests a potentially important effect of turbidity on pre-screen loss.

Covariates that predicted salvage efficiency improved fits to the salvage data, likely indicating that pre-screen loss in the CCF is sensitive to variation in a number of abiotic variables, perhaps because of their effects on biological processes such as concealment behavior and predation (Table 3). As described above, pre-screen loss declined with increases in turbidity (especially at the SWP); thus, the overall expansion factor decreased with increases

in turbidity. The turbidity-based model had much better predictive performance (lower AIC) than the constant pre-screen loss model, and had a much steeper slope at the SWP, resulting in an increase in the correlation (r^2) between observed and predicted salvage from 0.29 (constant) to 0.43 (turbidity). Of all the covariates we examined, export discharge has the smallest effect on pre-screen loss and model fit, resulting in a smaller decrease in AIC relative to the constant expansion factor model compared to the turbidity model. Increases in water temperature at Mallard led to higher salvage efficiency (lower pre-screen loss), but this model was not as good as the turbidity-based one. Unlike the turbidity response though, an improvement in fit occurred at both facilities. A model that included effects of both turbidity and export discharge produced a very similar fit to the turbidity-only model. However, a model with both turbidity and water temperature effects led to an improvement in fit, and its predictive ability (as indicated by lower AIC) was substantially better than the constant salvage expansion model. The turbidity and water-temperature model explained 42% of the variation in daily salvage at the CVP (compared to 27% for the constant efficiency model), and 63% of the variation at the SWP (compared to 29% for the constant efficiency model; Appendix A, Figure A1). Covariate efficiency models had a negligible effect on PEL, which is largely determined by unscaled PEL values from the behavior-movement models.

Three general patterns are evident in the comparison of all combinations of behavior-movement and population models. First, more complex behaviors fit the data much better compared to simpler BMMs. This is seen by lower ΔAIC values and higher rank order for more complex BMMs under the same population-model structure (moving down rows within columns in Table 2). A compact graphical comparison of the fit of all BMMs to the salvage data shows better fit of more complex behaviors at both the CVP and SWP (Figure A2). The improved fits of more complex BMMs do not incur an increase in the AIC parameter penalty (K in Equation 13) because the values in the movement array are treated as constants—and not parameters—in the population model. As a result, models with more complicated behaviors that fit the data better have lower AIC values and higher model ranks. A comparison of model fits using the familiar Pearson correlation coefficient is available in Appendix A (Table A1).

Second, the ranking of behavior-movement models did not depend on the population-model structure. However, within BMMs, increasing the complexity of the population model (moving from left to right in Tables 2 and A1) resulted in much better fits, and hence substantially lower AIC values. The addition of only one extra parameter to predict salvage efficiency as a function of turbidity (λ_1 in Equation 8B, population models 4 and 5) reduced AIC values by a few hundred points (Table 2), largely as a result of the improved fit to the SWP salvage data (Table 3). In conjunction with parameter estimates (Figure 7), this indicates very strong statistical support for turbidity-based variation in pre-screen loss at the SWP, but not at the CVP. Application of the model in other years is required to determine if this relationship actually reflects the effects of turbidity on salvage efficiency, or is an artifact caused by mis-timed predictions of entrainment from the BMMs. Predicting daily variation in natural survival rates as a function of model day lowered AIC values relative to the constant survival model (e.g., population model 1 vs. 2 and 4 vs. 5 in Table 2), but this difference was much less than the magnitude of the AIC reduction from using turbidity to predict salvage expansion factors. Predicting SKT sampling efficiency as a function of Secchi disc depth generally resulted in negligible changes to AIC, compared to models that assumed SKT sampling efficiency was constant (thus only varying with the ratio of tow and regional 4-m volumes). The only exception was for BMMs St and T. These latter models resulted in high densities in the most inland regions, which often had clear water (high Secchi depth) and low catch. As a result, the model could improve the fit to the SKT data by predicting a negative relationship between sampling efficiency and Secchi depth as estimated for juveniles captured in the FMWT surveys (Latour 2016). However, the improvement in fit was relatively

https://doi.org/10.15447/sfews.2021v19iss1art1

Table 3 Comparison of covariate models that predict salvage efficiency. Results are based on the TpsHt BMM, with logistically driven daily variation in natural survival rate (Sd) with no effect of Secchi disk depth on SKT sampling efficiency. The constant (Equation 8A) and turbidity (Equation 8B) models below are equivalent to population models 2 and 5, respectively in Table 2. Results show the estimated slopes for each covariate, the difference in AIC among models (relative to the constant model), and the amount of the daily variation in salvage explained by the model at the federal (CVP) and state (SWP) screening facilities (r^2). Also shown are proportional entrainment losses (PEL).

	slope (λ_1)		r^2			
Salvage Covariate Model	**CVP**	**SWP**	**CVP**	**SWP**	**ΔAIC**	**PEL**
Constant	NA	NA	0.27	0.29	0	0.34
Turbidity (Turb)	0.019	0.104	0.28	0.43	−360	0.35
Export Discharge (Q)	1.240	0.211	0.28	0.36	-56	0.34
Water Temperature (WT)	0.501	0.625	0.41	0.37	−196	0.33
Turb + Q	0.007, 1.293	0.100, 0.05	0.28	0.44	−367	0.35
Turb + WT	0.012, 0.438	0.113, 0.749	0.42	0.63	−589	0.35

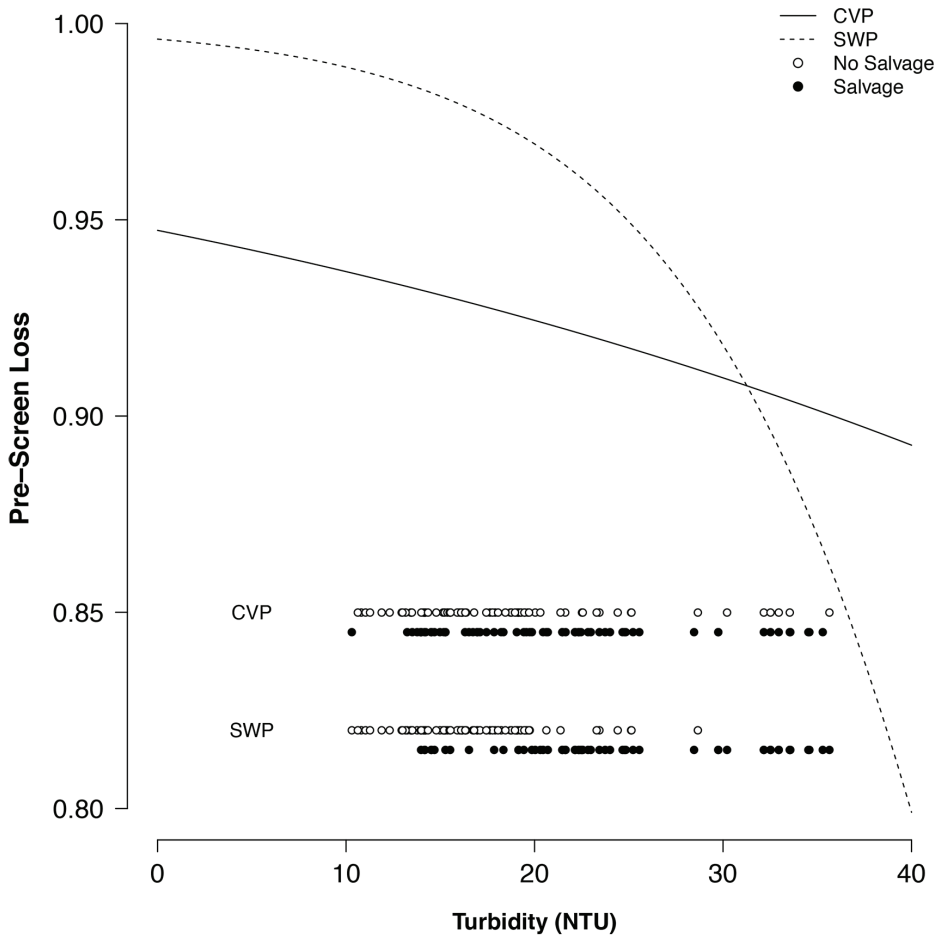

Figure 7 Predicted pre-screen loss–turbidity relationships for the federal (CVP, *solid line*) and state (SWP, *dashed line*) fish-screening facilities based on the TpsHt behavior model and population model 5 (see Table 2). Also shown are the daily turbidities when salvage was not observed (*open points*) or was observed (*closed points*).

modest, and still resulted in very high AIC and poor rank for these BMMs.

Finally, proportional entrainment loss estimates varied substantially across BMMs and negligibly across population models for a given BMM (Table 2). This indicates that movement predictions from the BMM (the **m** exchange array in Equation 4) dominate PEL estimates in the population model. This is also supported by the similarity between across-region unscaled PELs from the BMMs and those from the population models (Table 1) and the strong correlation between the two estimates. Variation in the magnitude of initial abundances across regions can influence PEL estimates, but the realized extent of this variation was limited through fitting to FMWT and SKT data. The best fit BMM (TpsHt) had a total PEL of 0.35 (CVP = 0.1, SWP = 0.25), and was higher than estimates from most other BMMs (except model T), largely because there were higher levels of entrainment from western and northern regions (Table 1). The trend in natural survival rate can also influence PEL, but estimates show a relatively high and constant rate through the end of January (Figure 3), which covers the majority of the period when entrainment of adult Delta Smelt occurred (Figure 6). Estimates of uncertainty in PEL values were unrealistically low (CV = 1.2%) because the predictions of movement were treated as constants in the statistical model.

DISCUSSION

Behavioral rules that incorporate concepts such as tidal surfing (Sommer et al. 2011), movement toward more turbid water (Bennett and Burau 2015), or movement toward less saline water (Rose et al. 2013) did not, on their own, do well at explaining the temporal and spatial variability in trawl catches or the temporal variation in salvage. More complex models that combined some of these behaviors and included lagged responses fit the data much better. Estimates of proportional entrainment loss varied considerably among BMMs, but were similar across alternate population-model structures within BMMs. The PEL estimate from the BMM and population model that fit the data from WY 2002 best was 35%, which is more than double the estimates of adult Delta Smelt PEL from Kimmerer 2008 and 2011 of 15% and 13%, respectively. Previous applications of our modeling framework using 2-D hydrodynamic simulations applied to data from water years 2002, 2004, and 2005 also produced PEL estimates about twice as high as Kimmerer's (2008) estimates (Korman et al. 2019). Our higher estimates of PEL are the result of behavioral assumptions in the BMMs, which lead to entrainment from regions that are further from the pumping facilities. Although the behavioral assumptions of the best-fit model presented here could misrepresent actual movements, the predictions of PEL do support Kimmerer's (2011) response to Miller's (2011) critique of his original paper, that "export-related losses to the Delta Smelt population during some of the years analyzed were substantial." The most pressing question for decision-makers is whether this conclusion is valid, and, more generally, whether the approach we have taken can be used to develop more reliable models that predict the effects of water export strategies on PEL compared to earlier efforts.

Factors Determining Differences in PEL and Salvage Expansion

Our estimates of PEL are higher compared to previously published estimates (Kimmerer 2008, 2011; Miller 2011) because movement predictions from the best-supported BMMs resulted in greater levels of proportional entrainment loss. The higher PEL predicted by the best-fitting models are in part caused by allowing particles to exhibit tidal migration behavior at some points during the simulation, which brings them closer to the pumps. To fit the salvage data, higher unscaled PELs from the BMM requires higher estimates of salvage expansion factors in the population model. This is most clearly illustrated using the equation

$$PEL \approx \frac{\mathbf{c_s} \cdot \theta_S^{-1}}{\mathbf{c_{SKT}} \cdot \theta_{SKT}^{-1}}. \quad (14)$$

The salvage ($\mathbf{c_s}$) and SKT ($\mathbf{c_{SKT}}$) data used here and in earlier studies are the same, and the SKT

https://doi.org/10.15447/sfews.2021v19iss1art1

expansion factors are also similar because they depend solely on measured tow volumes and the assumed 4-m habitat volume for Delta Smelt (θ_{SKT}^{-1}). Although there were some minor differences in the 4-m habitat volumes used in early studies and used here, it was mostly our larger estimate of PELs from the BMMs that required larger salvage expansion factors (θ_S^{-1}) to fit the data.

A review of previous estimates of salvage expansion factors and how they were determined will help put our approach of estimating PEL in context. Kimmerer estimated a salvage expansion factor by relating an estimated fish flux based on Kodiak trawl samples in the South Delta to the combined salvage at both fish screening facilities (see Equation 16 of Kimmerer 2008). The fish flux, which was an estimate of daily entrainment, was calculated as the catch per unit volume at four sampling stations multiplied by the mean daily combined flow rate (water volume per day) in Old and Middle rivers. The temporally-constant expansion factor, computed using multiple years of data, was then used to estimate annual PELs, given the observed annual salvage and estimated annual abundances across all regions (determined from the SKT survey data). Under this approach, the estimated salvage expansion factor is the leading parameter, and PEL was essentially calculated based on Equation 14 (assuming no natural morality effects). In contrast, with our approach, the BMM-based unscaled PEL is the leading parameter that determines the value of the salvage expansion factor.

Kimmerer (2008) estimated a mean salvage expansion value of 29 (95% confidence of 9 to 49) in his original analysis, and 22 (13 to 33) in his revised analysis (2011). Miller (2011) disputed these estimates on several grounds, arguing that they were biased high. In our view, all these estimates of the expansion factor are highly uncertain, largely because of uncertainty about whether the samples Kimmerer used in the South Delta to compute fish flux (entrainment) were adequate to represent the actual abundance. The fish flux was calculated by expanding very low catches from four tows collected monthly over 4 years of surveys (2002-2005) in the South Delta region (as defined in these earlier efforts). There are no data to support the assumption that Delta Smelt are distributed evenly to a depth of 4 m in both deep- and shallower-water habitats (Polansky et al. 2019), or that the vertical or horizontal distribution does not vary with abundance or other conditions such as turbidity, prey availability, or predator abundance. To our knowledge, there are no studies indicating that individual fish within a population are uniformly distributed, justifying the use of sampled volume-to-habitat ratios to convert catch to abundance. Kimmerer (2008, 2011) and Miller (2011) acknowledge the considerable uncertainty in PEL and salvage expansion factor estimates that arise from these assumptions. Their work has been helpful in advancing discussions and management of entrainment of Delta Smelt and other species. However, their salvage expansion factors do not provide a reliable standard to judge other values, such as the ones estimated in this study. Our model also depends on these same assumptions, but because the unscaled PEL from the BMM is the leading parameter in Equation 14, they only affect the estimated abundance and salvage expansion factors, and have little effect on PEL.

Field-based estimates of salvage expansion factors are more reliable than model-based ones because they depend less on highly uncertain assumptions. The proportion of entrained fish that are captured at fish screening facilities depends on the efficiency of the screens to salvage fish from the main flow before they reach the pumps (facility efficiency), and the proportion of entrained fish that die between the entrainment point and the screens (pre-screen loss). Castillo et al. (2012) released marked, cultured Delta Smelt just upstream of the screens at the SWP to measure facility efficiency, and at the entrance to the CCF to measure the total salvage efficiency from the CCF gates [(1 – pre-screen loss) × facility efficiency]. Based on releases in February and March 2009, total salvage efficiencies ranged from 0.4% to 3.1%, equivalent to salvage expansion factors of 32 (February) and 252 (March), respectively. Our mean SWP

expansion factor from the lowest AIC model (127) was comfortably within this range, as were the majority of daily estimates predicted as a function of turbidity. As explicitly stated by Castillo et al. (2012), salvage expansion factor estimates based on their March release experiments for adult Delta Smelt were about 10-fold higher than Kimmerer's values of 29 (2008) and 22 (2011). Mark-recapture experiments using cultured Delta Smelt have also been conducted at the CVP, with releases occurring at the intake channel (Bark et al. 2013; Sutphin and Svoboda 2016). Facility efficiency in the absence of predator removal averaged 0.20, which is equivalent to a salvage expansion factor of only 5, considerably lower than our estimate of 74. However, the mark-recapture-based estimate does not include pre-screen losses over the ~1-km channel between the CCF gates and the CVP intake (Figure 1), more extensive areas such as the Grand Canal and the Old River south of the CVP facility, or the South Delta as a whole. As discussed below, pre-screen loss is applied to any fish that is predicted to be entrained, which can occur at a considerable distance from the CCF gates and includes much of the South Delta. To resolve uncertainties associated with converting salvage observations to entrainment, additional mark-recapture experiments to estimate pre-screen loss as a function of distance to facility are critical. Smith (2019) also concluded that more field effort to estimate pre-screen loss is warranted.

Pre-Screen Loss

The spatial extent of pre-screen loss is uncertain and may be challenging to resolve for Delta Smelt. Castillo et al. (2012) quantified pre-screen loss in the CCF only (Figure 1). From a population closure perspective, this was a logical choice, because marked Delta Smelt released just inside the entrance of the gated forebay are unable to escape, thus ensuring that the entire marked population is vulnerable to entrainment. However, behavior-movement models indicate that most fish entering the South Delta region will be entrained, and entrainment rates for central and eastern regions can also be high. Acoustic and coded-wire tagging studies for juvenile Chinook Salmon demonstrate that survival is very low in the Central and South Delta because of high rates of predation (Buchanan et al. 2018), and predation losses are expected to be even higher for Delta Smelt (Grossman 2016). Our salvage expansion factors apply to any particle which is entrained, and should therefore include the effect of higher predation-driven mortality in the central and southern regions of the Delta. We did not estimate region-specific natural survival rates in the population model. This would have increased the computational time of the population dynamics model by about four orders of magnitude. More importantly, allowing both temporal and spatial variation in survival would put an even greater demand on the sparse SKT data to estimate these parameters (see discussion below). Our estimates of salvage expansion factors could be implicitly accounting for the higher mortality rate in Central and South Delta, which was not explicitly modeled. But they could also be compensating for predictions of entrainment that are too high, though our comparison with the limited number of mark-recapture-based estimates of salvage expansion do not suggest this is the case. We would expect our estimates of salvage expansion to be considerably higher than estimates in Castillo et al. (2012) because they cover the entire area over which entrainment occurs, rather than just the CCF. Given a choice between assuming no pre-screen loss for fish entrained upstream of the CCF gates or the CVP intake channel, or substantial losses as our results suggest, the available evidence on predator abundance and predation rates provides more support for the assumption used in this analysis. Testing this critical assumption, by quantifying the extent of pre-screen loss upstream of CCF, will be somewhat challenging because of uncertainty in the proportion of marked fish that can potentially escape the entrainment field. Passive Integrative Transponder (PIT)-tagging of Delta Smelt is feasible, and the continuing reductions in the size of acoustic and radio tags may eventually allow adult Delta Smelt to be tracked (Wilder et al. 2016). These tagging methods can be used in tandem to estimate pre-screen loss over larger areas.

https://doi.org/10.15447/sfews.2021v19iss1art1

We estimated that the salvage expansion was considerably higher when the water was clearer, especially at SWP, where entrained fish must pass through the CCF. Two possible mechanisms could be driving this relationship. If the modeled daily predictions of entrainment loss are accurate, the relationship could be quantifying the increase in predation-related pre-screen loss that occurs when the water is clear compared to when it is turbid (turbidity-predation loss hypothesis). Alternatively, the BMMs may be failing to capture turbidity-related movement behavior over shorter time-scales, and the turbidity-salvage expansion relationship could be compensating for this limitation (turbidity-movement hypothesis). For example, if Delta Smelt spent more time concealing themselves near the bottom or the edges of the channel when the water was clear, they would be less vulnerable to entrainment. This effect could be much stronger in CCF because it is shallow and has a very high concentration of predators (Grossman 2016), which is consistent with our results of a much stronger turbidity-salvage expansion relationship at the SWP than at the CVP. There is considerable evidence from other systems to support both turbidity-predation (Ginetz and Larkin 1976; Gregory and Levings 1998; Johnson and Hines 1999; Yackulic et al. 2017; Yard et al. 2011) and turbidity-movement hypotheses (Gradall and Swenson 1982; Guthrie and Muntz 1993; Miner and Stein 1996; Korman et al. 2016; Korman and Yard 2017). They are both likely driven by the same behavior, because lower predation risk associated with higher turbidity would reduce concealment behavior, which in turn would increase the probability that fish are drawn toward the pumps and entrained. The turbidity-movement hypothesis is a potential mechanism that explains the increase in Delta Smelt salvage shortly after the "first flush" when turbidity increases (Grimaldo et al. 2009, this volume).

Limitations of the Model

Our estimates of differences in AIC among BMMs were large, erroneously implying a high degree of certainty in identifying the best BMM. Given large differences in PEL from different BMMs, this result also erroneously implies high confidence in PEL estimates. These conclusions are an artifact of our two-step modeling procedure, where the BMM is first used to calculate a large movement array whose values are then treated as fixed parameters with no uncertainty in the population model. This strategy was necessary because the BMM simulation is much too slow to run in an optimization environment to jointly fit movement and population parameters. If behavioral parameters could be estimated this way, there would be many alternative combinations of values that fit the data well—some of which could have very different PELs. This would lead to higher and more realistic variance estimates for PEL within BMMs, and much smaller differences in AIC among alternative BMMs that may have very different PELs. In addition, limitations in data did not allow us to include process error in population-model predictions, which would also lead to over-estimates of certainty in PEL. Because of these issues, results presented here only roughly characterize the degree of statistical support for various levels of proportional entrainment loss. The more complex and integrated structure in the original Delta Smelt life-cycle model (Newman et al. 2014) potentially addressed many of these limitations, but fitting this model was problematic because of data limitations. Future modeling work could explore options for directly estimating movement parameters in an optimization environment, perhaps by compromising between the complex structure of Newman et al.'s life-cycle model and the much simpler one used here. Limiting the number of spatial regions, use of cloud computing, and developing more efficient ways of drawing parameters during optimization (Noble et al. 2017) are potential approaches to explore in a fully integrated behavioral movement-population model.

Confidence in PEL predictions could also be increased using our two-stage modeling framework, but fitting to multiple years of data at the same time (joint estimation). Population model parameters could be estimated using a mixed-effects model, with each year treated as a random effect for parameters such as natural survival

rate or salvage expansion factors. Confidence in estimates of the salvage expansion-turbidity relationship would increase if relationships were similar across years. A joint-estimation approach would also identify the BMM that provides the best fit to multiple years of data, and describe how the fit varies across years. When we applied our modeling framework separately to 4 water years (2002, 2004, 2005, and 2011) using 2-D hydrodynamics, a different best-fit BMM was identified for 3 of the 4 years, and in some cases, this made a substantial difference in PEL. Cross-validation approaches, where 1 or more years of data is left out of the fitting and instead used to test predictions, could be used to better evaluate the out-of-sample predictive ability of the models. In our view, these types of multi-year assessment are essential if the modeling framework is to be used by decision-makers to evaluate export strategies. A joint-estimation approach would not be very difficult to implement for the population model described in this paper, and would have similarities to the method developed by Smith (2019) to estimate annual entrainment. However, decisions on further modeling investments should consider that estimates of uncertainty in PEL from such efforts may still be greater than managers prefer for making difficult trade-off decisions.

A multi-year, joint-estimation approach would also allow us to determine whether annual variation in PEL is consistent with the relationship between juvenile and adult Delta Smelt abundance among years. For example, a high and variable pattern in PEL across years is not consistent with the observation that there is a strong correlation ($r^2 = 0.91$) between juvenile abundance estimated from the FMWT surveys (in log space) and the adult abundance in February estimated from the SKT surveys (IEP MAST 2015). That strong correlation may be an artifact of biased population estimates, because the correlation based on more recent estimates (Polanksy et al. [2019] was much lower, r^2=0.61; 2019 email from William E. Smith sent to JK and others on July 7, unreferenced; see "Notes"). Bootstrapping procedures that incorporated uncertainty in abundance estimates also demonstrated that the observed FMWT-SKT correlation is consistent with the sometimes high and variable PEL estimates that Smith et al. (2018) calculated. Inferences from such analyses could be improved by reformulating the FMWT-SKT relationship into a stock-recruitment relationship and incorporating it in our modeling framework in a multi-year application. BMMs that predict annual PELs which are not consistent with the stock-recruit relationship would be penalized accordingly. This would be a useful analysis for decision-makers, because it would replace binary arguments about whether the estimated PEL times series is "right" or "wrong" based on inconsistent treatments of the data, where uncertainty in only some of the components is recognized.

Limitations in the Data Used to Fit Models

Fitting models to data provides a consistent way to evaluate alternative hypotheses, but, just as importantly, also provides an improved understanding of the data and its limitations. Currently, annual abundance estimates of adult Delta Smelt are based on two of the five SKT surveys available per year, with about 40 stations sampled per survey (Polansky et al. 2019). Our modeling effort asks much more specific questions about the abundance of the population in any year, and therefore asks much more from the same SKT data. For example, in the water year 2002 application, the model predicts abundance for each of three surveys in 15 regions. The same data used to fit one estimate of annual abundance for water year 2002 (based on February and March surveys in Polansky et al. 2019) now needs to support 30 different estimates in our model over that same time-period (15 regions * 2 surveys). Not surprisingly, inferences from this more thinly-sliced data are weaker. Consider, as an example, entrainment predictions of Delta Smelt after the first flush, when the majority of adults are salvaged (Grimaldo et al. 2009). The prediction depends in part on the size of the population in the South Delta at that time. The model estimated a catch of 4.5 fish per tow during the January 2002 survey, which in an absolute sense is less than two fish more than the three-station mean of 2.7 fish per tow. But in a relative sense this implies the model has over-

https://doi.org/10.15447/sfews.2021v19iss1art1

estimated the expected abundance in the South Delta by about 65%, leading to the conclusion that entrainment has also been potentially over-estimated by this amount (if one also ignores over-estimation of abundance in western regions for the purpose of this argument). However, catch rates vary widely across the different stations sampled in a region within surveys, likely as a result of extensive variation in fish density and, perhaps, catchability (Latour 2016). High sampling variance (e.g., a 10:1 variance-to-mean ratio in water year 2002) leads to a relatively small reduction in the likelihood of the data by estimating an expected value of 4.5 rather than 2.7 fish per tow. In other words, there is only limited statistical support for the conclusion that predicted abundance in the South Delta, and hence PEL is biased high because the penalty in the likelihood of not perfectly predicting the sparse catch data is low. The model we have developed accounts for uncertainty in Delta Smelt abundance over space and time, and in this respect is an improvement over past PEL estimation efforts, which have treated abundance as perfectly determined values. Recently published estimates of uncertainty in SKT-derived abundance estimates for adult Delta Smelt (Polansky et al. 2019) will likely be influential in moving away from deterministic use of abundance estimates. Interestingly, that study estimated that the average CV for annual abundance estimates of adult Delta Smelt, based on combining data from February and March surveys, was 31%. Much higher levels of variability are expected for region- and survey-specific estimates, such as those needed for this analysis. Thus, there is very limited information to determine if our best model over-estimated abundance in the South Delta. Deficiencies in the information content of SKT data would also severely limit the ability to estimate variation in survival rates among regions, even if computational costs were not an issue.

Evaluating the effects of entrainment on the viability of the Delta Smelt population is challenging and may be difficult to achieve. We have reviewed many of the issues that lead to uncertainty in proportional entrainment loss. Additional modeling and field efforts can reduce uncertainty in PEL estimates to some extent, but the effect of PEL on population viability will depend on its productivity, which will remain difficult to quantify given the available data, though attempts have been made (Maunders and Deriso 2011; Rose et al. 2013). In addition, the severe declining trend in abundance indices (Moyle et al. 2016; Polansky et al. 2018) almost certainly indicates that natural levels of productivity for Delta Smelt are much lower since the Pelagic Organism Decline (Sommer et al. 2007; Mac Nally et al. 2010). Just as more productive salmon populations can support higher maximum sustainable yields and exploitation rates, a more productive Delta Smelt population can withstand higher levels of entrainment and PEL and still be viable. It is uncertain whether the current USFWS RPA in the Biological Opinion for Delta Smelt (USFWS 2008), which reduces water exports and is predicted to reduce PEL based on the models presented here (Gross et al. 2018; Appendix C), has effectively reduced PELs to levels non-detrimental to population recovery. Because of data limitations, estimates of the effects of water exports on population viability for Delta Smelt will likely always be uncertain. Given this situation, methods that provide more reliable measures of factors that affect salvage (Grimaldo et al., this volume), or models that provide improved estimates of total entrainment (Smith 2019), or proportional entrainment loss, such as the one presented here, are useful tools to help managers make very difficult choices on water exports in the Delta.

ACKNOWLEDGMENTS

Funding for this study was provided by the United States Bureau of Reclamation, State and Federal Contractors Water Agency, and the California Department of Water Resources through the Collaborative Science Adaptive Management Program. This study was done under the direction of CSAMP's Collaborative Adaptive Management Team (CAMT) and the Delta Smelt Scoping Team (DSST). We would like to thank Ken Newman, Leo Polansky, and William Smith for providing much of the data used in our

analysis and for many insightful conversations over the course of this project. Our analysis relied heavily on long-term trawl and salvage data sets. We thank the many biologists and technicians working for the California Department of Fish and Wildlife, the US Fish and Wildlife Service, and the US Bureau of Reclamation for the collection and maintenance of these data. We thank the DSST and Matt Nobriga for providing valuable comments and discussion over the course of this project and on earlier drafts of this manuscript. We thank three anonymous reviewers for their helpful comments. The findings and conclusions of this study are those of the authors and do not necessarily represent the views of our respective agencies.

REFERENCES

Ahrestani FS, Hebblewhite M, Post E. 2013. The importance of observation versus process error in analyses of global ungulate populations. Sci Rep. [accessed 2020 Jan 08];3:3125. *https://doi.org/10.1038/srep03125*

Barnthouse LW, Kladua RJ, Vaughan DS, Kendall RL. 1988. Science, law, and Hudson River power plants: a case study in environmental impact assessment. Am Fish Soc Mon 4. American Fisheries Society, Bethesda, Maryland, USA. 346 p.

Bark RC, Bridges B, Bowen MD. 2013. Predator impacts on salvage rates of juvenile Chinook Salmon and Delta Smelt. United States Department of the Interior, US Bureau of Reclamation. Tracy Technical Bulletin 2013-1.

Bennett WA. 2005. Critical assessment of the Delta Smelt population in the San Francisco Estuary, California. San Franc Estuary Watershed Sci. [accessed 2021 Jan 08];3(2). *https://doi.org/10.15447/sfews.2005v3iss2art1*

Bennett WA, Burau JR. 2015. Riders on the storm: Selective tidal movements facilitate the spawning migration of threatened Delta Smelt in the San Francisco Estuary. Estuaries Coast. [accessed 2021 Jan 08];38:826–835. *https://doi.org/10.1007/s12237-014-9877-3*

Brown LR, Kimmerer W, Brown R. 2009. Managing water to protect fish: a review of California's environmental water account, 2001-2005. Environ Manage. [accessed 2021 Jan 08];43:357-368. *https://doi.org/10.1007/s00267-008-9213-4*

Blumberg AF, Dunnin DJ, Li H, Heimbuch D, Geyer WR. 2004. Use of a particle-tracking model for predicting entrainment at power plants on the Hudson River. Estuaries. [accessed 2021 Jan 08];27:515–526. *https://doi.org/10.1007/BF02803543*

Buchanan RA, Brandes BL, Skalski JR. 2018. Survival of juvenile fall-run Chinook salmon through the San Joaquin River Delta, California, 2010-2015. Nor Am J of Fish Manage. [accessed 2021 Jan 08];38:663-679. *https://doi.org/10.1002/nafm.10063*

Burnham KP, Anderson DR. 2002. Model selection and multimodel inference. (2nd ed.) New York (NY): Springer-Verlag.

[CDWR] California Department of Water Resources. 2019. Dayflow. Environmental planning and information branch, Dayflow Program. [accessed 2019 Oct 03]. Available from: *https://water.ca.gov/Programs/Environmental-Services/Compliance-Monitoring-And-Assessment/Dayflow-Data*

Castillo G, Morinaka J, Lindberg J, Fujimura R, Baskerville-Bridges B, Hobbs J, Tigan G, Ellison L. 2012. Pre-screen loss and fish facility efficiency for Delta Smelt at the South Delta's State Water Project, California. San Franc Estuary Watershed Sci. [accessed 2021 Jan 08];10(4). *https://doi.org/10.15447/sfews.2012v10iss4art4*

Culberson SD, Harrison CB, Enright C, Nobriga ML. 2004. Sensitivity of larval fish transport to location, timing, and behavior using a particle tracking model in Suisun FeyMarsh, California. Am Fish Soc Symp 39:257-267.

Feyrer F, Nobriga M, Sommer T. 2007. Multi-decadal trends for three declining fish species: habitat patterns and mechanisms in the San Francisco Estuary, California, USA. Can J Fish Aquat Sci. [assessed 2021 Jan 08];64:723–734. *https://doi.org/10.1139/f07-048*

Feyrer F, Portz D, Odum D, Newman KB, Sommer T, et al. 2013. Correction: SmeltCam: Underwater video codend for trawled nets with an application to the distribution of the imperiled Delta Smelt. PLoS ONE [accessed 2021 Jan 25];8(12). *https://doi.org/10.1371/annotation/0c42ea0f-6d99-44a7-84ff-aeec57133f13*

Fournier DA, Skaug HJ, Ancheta J, Ianelli J, Magnusson A, Maunder MN, Nielsen A, Sibert J. 2011. AD Model Builder: using automatic differentiation for statistical inference of highly parameterized complex nonlinear models. Optimization Methods & Software. [accessed 2012 Feb 17]. Available from: *http://admb-project.org/*

Ginetz RM, Larkin PA. 1976. Factors affecting Rainbow Trout (*Salmo gairdneri)* predation outmigrant fry of Sockeye Salmon (*Oncorhynchus nerka*). J Fish Res Board Can 33:19–24.

Gradall KS, Swenson WA. 1982. Response of Brook Trout and Creek Chubs to turbidity. Trans Am Fish Soc. [accessed 2021 Jan 08];111:392–395. *https://doi.org/10.1577/1548-8659(1982)111%3C392:ROBTAC%3E2.0.CO;2*

Gregory RS, Levings CD. 1998. Turbidity reduces predation on migrating juvenile Pacific Salmon. Trans Am Fish Soc. [accessed 2021 Jan 08];127:275–285. *https://doi.org/10.1577/1548-8659(1998)127%3C0275:TRPOMJ%3E2.0.CO;2*

Grimaldo L, Sommer T, Van Ark N, Jones G, Holland E, Moyle P, Herbold B, Smith P. 2009. Factors affecting fish entrainment into massive water diversions in a freshwater tidal estuary: can fish losses be managed? Nor Am J Fish Manage. [accessed 2021 Jan 08];29:1253-1270. *https://doi.org/10.1577/M08-062.1*

Gross ES, Korman J, Grimaldo L, MacWilliams ML. 2019. Evaluation of hypothesized adult Delta Smelt swimming behaviours. San Franc Estuary Watershed Sci, this volume.

Gross ES, Saen, B, Rachiele R, Grinbergs S, Grimaldo LF, Korman J, Smith PE, MacWilliams M, Bever A. 2018. Estimation of adult Delta Smelt distribution for hypothesized swimming behaviors using hydrodynamic, suspended sediment and particle-tracking models. Technical Report DWR 1249. Resource Management Associates Technical Report, Collaborative Adaptive Management Team. [accessed 2021 Jan 08]; 58 p. Available from: *https://www.waterboards.ca.gov/waterrights/water_issues/programs/bay_delta/california_waterfix/exhibits/docs/petitioners_exhibit/dwr/part2_rebuttal/dwr_1249.pdf*

Gross ES, Korman J, Grimaldo LF, MacWilliams ML, Bever AJ, Smith PE. 2021. Modeling Delta Smelt distribution for hypothesized swimming behaviors. San Franc Estuary Watershed Sci. *https://doi.org/10.15447/sfews.2021v19iss1art3*

Grossman GD. 2016. Predation of fishes in the Sacramento-San Joaquin Delta: current knowledge and future directions. San Franc Estuary Watershed Sci. [accessed 2021 Jan 08];14(2). *https://doi.org/10.15447/sfews.2016v14iss2art8*

Guthrie DM, Muntz WRA. 1993. Role of vision in fish behaviour. In: Pitcher TJ, editor. Behavior of Teleost Fishes. (London): Chapman and Hall. Pages 89–121

Heimbuch DG, Dunning DJ, Ross QE, Blumberg AF. 2007. Assessing potential effects of entrainment and impingement on fish stocks of the New York–New Jersey Harbor estuary and Long Island Sound. Trans Am Fish Soc. [accessed 2021 Jan 08];136:492–508. *https://doi.org/10.1577/T06-090.1*

Hinrichsen HH, Dickey-Collas M, Huret M, Peck MA, Vikebø FB. 2011. Evaluating the suitability of coupled biophysical models for fishery management. ICES J Mar Sci. [accessed 2021 Jan 08];68:1478-1487. *https://doi.org/10.1093/icesjms/fsr056*

[IEP MAST] Interagency Ecological Program Management, Analysis, and Synthesis Team. 2015. An updated conceptual model for Delta Smelt: our evolving understanding of an estuarine fish. Sacramento (CA): California Department of Water Resources. [accessed 2021 Feb 12]; 223 p. Avalable from: *https://www.waterboards.ca.gov/waterrights/water_issues/programs/bay_delta/california_waterfix/exhibits/docs/petitioners_exhibit/dwr/part2/DWR-1089%20IEP_MAST_Team_2015_Delta_Smelt_MAST_Synthesis_Report_January%202015.pdf*

[ICOLD] International Commission on Large Dams. World Register of Dams—general synthesis. 2015. [accessed 2016 Nov 24]. Available from: *http://www.icold-cigb.net/GB/World_register/general_synthesis.asp*

Johnson JD, Hines RT. 1999. Effect of suspended sediment on vulnerability of young Razorback Suckers to predation. Trans Am Fish Soc. [accessed 2021 Jan 08];128:648–655. *https://doi.org/10.1577/1548-8659(1999)128%3C0648:EOSSOV%3E2.0.CO;2*

Kimmerer WJ. 2004. Open water processes of the San Francisco Estuary: from physical forcing to biological responses. San Franc Estuary Watershed Sci. [accessed 2021 Jan 08];2(1). *https://doi.org/10.15447/sfews.2004v2iss1art1*

Kimmerer WJ. 2008. Losses of Sacramento River Chinook Salmon and Delta Smelt to entrainment in water diversions in the Sacramento-San Joaquin Delta. San Franc Estuary Watershed Sci. [accessed 2021 Jan 08]; 6(2). *https://doi.org/10.15447/sfews.2008v6iss2art2*

Kimmerer WJ, Nobriga ML. 2008. Investigating particle transport and fate in the Sacramento-San Joaquin Delta using a particle tracking model. San Franc Estuary Watershed Sci. [accessed 2021 Jan 08];6(1). *https://doi.org/10.15447/sfews.2008v6iss1art4*

Kimmerer WJ. 2011. Modeling Delta Smelt losses at the South Delta export facilities. San Franc Estuary Watershed Sci. [accessed 2021 Jan 08];9(1). *https://doi.org/10.15447/sfews.2011v9iss1art3*

Korman J, Gross ES, Smith PE, Saenz B, Grimaldo LF. 2019. Statistical evaluation of particle-tracking models prediction proportional entrainment loss for adult Delta Smelt in the Sacramento-San Joaquin Delta. April 11, 2018. [acessed 2020 Nov 11]; 111 p. Available from: *https://www.waterboards.ca.gov/waterrights/water_issues/programs/bay_delta/california_waterfix/exhibits/docs/petitioners_exhibit/dwr/part2_rebuttal/dwr_1259.pdf*

Korman J, Yard MD, Yackulic CB. 2016. Factors controlling the abundance of Rainbow Trout in the Colorado River in the Grand Canyon in a reach utilized by endangered Humpback Chub. Can J Fish Aquat Sci. [accessed 2021 Jan 08];73:105-124. *https://doi.org/10.1139/cjfas-2015-0101*

Korman J, Yard MD. 2017. Effects of environmental covariates and density on the catchability of fish populations and the interpretation of catch per unit effort trends. Fish. Res. [accessed 2021 Jan 08];189:18-34. *https://doi.org/10.1016/j.fishres.2017.01.005*

Latour RJ. 2016. Explaining patterns of pelagic fish abundance in the Sacramento-San Joaquin Delta. Estuaries Coasts. [accessed 2021 Jan 08];39:233-247. *https://doi.org/10.1007/s12237-015-9968-9*

Mac Nally R, Thomson JR, Kimmerer WJ, Feyrer F, Newman KB, Sih A, Bennett WA, Brown L, Fleishman E, Culberson SD et al. 2010. Analysis of pelagic species decline in the upper San Francisco Estuary using multivariate autoregressive modeling (MAR). Ecol App. [accessed 2021 Jan 08];20:1417-1430. *https://doi.org/10.1890/09-1724.1*

Maunder MN, Deriso RB. 2011. A state-space multistage life cycle model to evaluate population impacts on the presence of density dependence: illustrated with application to Delta Smelt (Hypomesus transpacificus). Can J Fish Aquat Sci. [accessed 2021 Jan 08];68:1285-1306. *https://doi.org/10.1139/f2011-071*

Miner JG, Stein RA. 1996. Detection of predators and habitat choice by small bluegills: effects of turbidity and alternative prey. Trans Am Fish Soc. [accessed 2021 Jan 08];125:97–103. *https://doi.org/10.1577/1548-8659(1996)125%3C0097:DOPAHC%3E2.3.CO;2*

Miller WJ. 2011. Revisiting assumptions that underlie estimates of proportional entrainment of Delta Smelt by state and federal water diversions from the Sacramento-San Joaquin Delta. San Franc Estuary Watershed Sci. [accessed 2021 Jan 08];9(1). *https://doi.org/10.15447/sfews.2011v9iss1art2*

Moyle PB, Brown LR, Durand JR, Hobbs JA. 2016. Delta Smelt: life history and decline of a once-abundant species in the San Francisco Estuary. San Franc Estuary Watershed Sci. [accessed 2021 Jan 08];4(2). *https://doi.org/10.15447/sfews.2016v14iss2art6*

Newman KB, Polansky L, Mitchell L, Kimmerer W, Smith P, Baxter R, Bennet W, Mander M, Nobriga M, Meiring W, et al. 2014. A Delta Smelt life cycle model. Draft report prepared by USFWS Dec 17, 2014.

Noble H, Jennings E, Criss A, Danner E, Sridharan V, Greene CM, Imaki H, Lindley ST. 2017. Model description for the Sacramento River winter-run Chinook Salmon life cycle model. May 9, 2017. [accessed 2019 Feb 02]: 49 p. Available from: *https://www.noaa.gov/sites/default/files/atoms/files/0.7.115.5947-000001.pdf*

North EW, Schlag Z, Hood RR, Li M, Zhong L, Gross T, Kennedy VS. 2008. Vertical swimming behavior influences the dispersal of simulated oyster larvae in a coupled particle-tracking and hydrodynamic model of Chesapeake Bay. Mar Ecol Prog Ser. [accessed 2021 Jan 08];359:99–115. *https://doi.org/10.3354/meps07317*

Polansky L, Mitchell L, Newman KB. 2019. Using multistage design-based methods to construct abundance indices and uncertainty measures for Delta Smelt. Trans Am Fish Soc. [accessed 2021 Jan 08];148:710-724. *https://doi.org/10.1002/tafs.10166*

Polansky L, Newman KB, Nobriga ML, Mitchell L. 2018. Spatiotemporal models of an estuarine fish species to identify patterns and factors impacting their distribution and abundance. Estuaries Coasts. [accessed 2021 Jan 08];41:572–581. *https://doi.org/10.1007/s12237-017-0277-3*

Rose KA, Kimmerer WJ, Edwards KP, Bennett WA. 2013. Individual-based modeling of Delta Smelt population dynamics in the upper San Francisco Estuary: I. Model description and baseline results. Trans Am Fish Soc. [accessed 2021 Jan 08];142:1238–1259. *https://doi.org/10.1080/00028487.2013.799518*

Rytwinski T, Algera DA, Taylor JJ, Smokorowski KE, Bennett JR, Harrison PM, Cooke SJ. 2017. What are the consequences of fish entrainment and impingement associated with hydroelectric dams on fish productivity? a systematic review protocol. Environ Evid. [accessed 2021 Jan 08];6:8. *https://doi.org/10.1186/s13750-017-0087-x*

Simpson WG. 2018. The entrainment and screening of returning and postspawning adult salmonids at irrigation canals of the Umatilla River, Oregon. J Fish Wildl Manag. [accessed 2021 Jan 08];9:285-295. *https://doi.org/10.3996/072017-JFWM-058*

Smith W. 2019. Integration of transport, survival, and sampling efficiency in a model of South Delta entrainment. San Franc Estuary Watershed Sci. [accessed 2021 Jan 08];17(4). *https://doi.org/10.15447/sfews.2019v17iss4art4*

Smith PE, Donovan JM, Gross ES, Korman J, McNamara BJ, Grimaldo LF. 2018. Adult Delta Smelt proportional entrainment losses at state and federal export facilities in the Sacramento-San Joaquin Delta. Report prepared for the Collaborative Science Adaptive Management Program for the Sacramento-San Joaquin Delta (draft). December 11, 2018.

Sommer T, Mejia F, Nobriga M, Feyrer F, Grimaldo L. 2011. The spawning migration of Delta Smelt in the upper San Francisco Estuary. San Franc Estuary Watershed Sci. [accessed 2021 Jan 08];9(2). *https://doi.org/10.15447/sfews.2014v9iss2art2*

Sommer T, Armor C, Baxter R, Breuer R, Brown L, Chotkowski M, Culberson S, Feyrer F, Gingras M, Herbold B, et al. 2007. The collapse of pelagic fishes in the upper San Francisco Estuary. Fisheries. [accessed 2021 Jan 08];32:270-277. *https://doi.org/10.1577/1548-8446(2007)32[270:TCOPFI]2.0.CO;2*

Sutphin ZA, Svoboda CD. 2016. Effects of hydraulic conditions on salvage efficiency of adult Delta Smelt at the Tracy Fish Collection Facility. United States Department of the Interior, Bureau of Reclamation, Tracy Series 43. [accessed 2020 Nov 11]. Available from: *https://www.usbr.gov/mp/TFFIP/////docs/tracy-reports/tracy-rpt-vol-43-effects-hydraulic.pdf*

Thomson JR, Kimmerer WJ, Brown LR, Newman KB, Mac Nally R, Bennett WA, Feyrer F, Fleishman E. 2010. Bayesian change point analysis of abundance trends for pelagic fishes in the upper San Francisco Estuary. Ecol Appl. [accessed 2021 Jan 08];20(5):1431–1448. *https://doi.org/10.1890/09-0998.1*

[USFWS] US Fish and Wildlife Service. 2008. 2008 Biological Opinion for Delta Smelt. [accessed 2021 Jan 08]; 65 p. Available from: *https://www.fws.gov/sfbaydelta/documents/SWP-CVP_OPs_BO_12-15_final_OCR.pdf*

[USFWS] US Fish and Wildlife Service. 2017. Enhanced Delta Smelt monitoring. Preliminary abundance analysis (draft), March 31, 2017. [accessed 2020 Nov 11]; 22 p. Available from: *https://www.fws.gov/lodi/juvenile_fish_monitoring_program/data_management/EDSM_report_2017_07_21.pdf*

Wanger OW. 2007. Findings of fact and conclusions of law re interim remedies are: Delta Smelt ESA remand and reconsultation. Case 1: 05-cv-01207-OWW-GSA. Document 561. Fresno (CA): United States District Court, Eastern District of California, [accessed 2021 Jan 08]; 45 p. Available from: *https://www.fws.gov/sfbaydelta/cvp-swp/Archives/documents/OCAP_Court_Finding_of_Fact_12-14-07.pdf*

Wanger OW. 2010. Memorandum decision re. Cross motions for summary judgment. Case 1: 09-cv-00407-OWW-DLB. Document 561. United States District Court, Eastern District of California, Fresno, California, USA. [accessed 2021 Jan 08]; 225 p. Available from: *https://www.endangeredspecieslawandpolicy.com/assets/htmldocuments/blog/4/2013/12/Docket-757-Memo-Decision-re-Cross-Motions-for-Su1.pdf*

White JW, Nickols KJ, Clarke L, Largier JL. 2010. Larval entrainment in cooling water intakes: spatially explicit models reveal effects on benthic metapopulations and shortcomings of traditional assessments. Can J Fish Aquat Sci. [accessed 2021 Jan 08];67: 2014–2031. *https://doi.org/10.1139/F10-108*

Wilder RM, Hassrick JL, Grimaldo LF, Greenwood MFD, Acuna S, Burns JM, Maniscalco DM, Crain PK, Hung TC. 2016. Feasibility of passive integrated transponder and acoustic tagging for endangered adult Delta Smelt. Nor Am J Fish Manage. [accessed 2021 Jan 08];36:1167-1177. *https://doi.org/10.1080/02755947.2016.1198287*

Yackulic CB, Korman J, Yard MD, Dzul M. 2017. Inferring species interactions through joint mark-recapture analysis. Ecology. [accessed 2021 Jan 08];99:812-821. *https://doi.org/10.1002/ecy.2166*

Yard MD, Coggins LG Jr, Baxter CV, Bennett GE, Korman J. 2011. Trout piscivory in the Colorado River, Grand Canyon: effects of turbidity, temperature, and fish prey availability. Trans Am Fish Soc. [accessed 2021 Jan 08];140:471-486. *https://doi.org/10.1080/00028487.2011.572011*

NOTES

Smith, William E. 2019. Email from WES, US Fish and Wildlife Service, to JK, Delta Smelt Scoping Team, and others dated July 07, 2019, entitled: "Evidence for bias in Study 3 PELs." Available from: *william_e_smith@fws.gov*.

https://doi.org/10.15447/sfews.2021v19iss1art1